Regenerative effects of notochordal cell matrix (NCM) on degenerated canine intervertebral discs (IVDs) *in vivo*

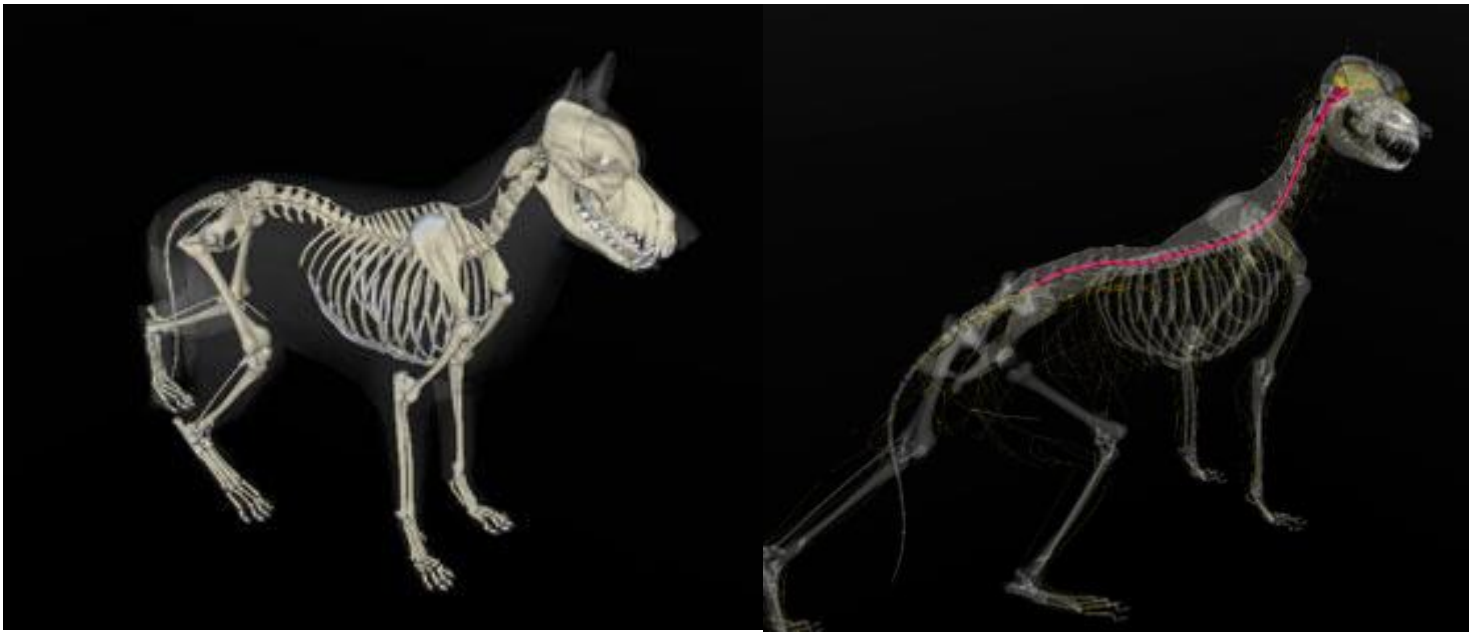

Author:	Amber van Heezen
Student number:	3574857
Timeslot:	June 2017 – October 2017
Location:	Utrecht University – Veterinary medicine
Department	Companion animals
Research group:	Orthopedics
Supervisors:	Drs. F.C. (Frances) Bach
	Dr. M.A. (Marianna) Tryfonidou
	Drs. M. (Martijn) Beukers

Utrecht University

Index

Abstract

Introduction: Intervertebral disc (IVD) degeneration is a progressive condition, which is common in dogs and humans. Symptom-oriented treatments are available to alleviate the pain, but not to reverse degeneration of the IVD. IVD degeneration is diagnosed by using magnetic resonance imaging, whereby the disc height index (DHI) can be measured. Also, new sequences, New techniques like T1ρ and T2 mapping are used to expose early degenerative changes in the IVD.
Because only symptom-oriented treatments are available, the interest to resolve the degeneration has gained interest over the years. Cell therapies have potential regenerative effects, whereby mesenchymal stromal cells (MSCs) and notochordal cells (NCs) have shown to have anabolic and stimulatory effects on nucleus pulposus cells NPCs. It is difficult to identify the NC secreted factors with a notochordal cell conditioned medium (NCCM) and thereby a new approach is being researched, namely notochordal cell matrix (NCM). Positive results are found *in vitro*, but the long-term effects have not been determined yet *in vivo*. Thereby the aim of this study is to determine whether effects of NCM treatment are observed at MRI (T1ρ, T2 mapping, DHI) and protein expression level (collagen type I, II, X, COX-2) and if MSC treatment can exert an additive effect.
Materials and methods: Five Beagles were used in this study, whereby degeneration was induced in the IVDs six weeks before the start of the treatments. Different treatments were given at T= 0 months, including NCM, MSC and NCM+MSC treatment and a reinjection of NCM at T=3 months was given in one group (2x NCM). Also, a control group and a group with induction but without treatments were used. MRIs were made at T= 0 months, T=3 months and T=6 months and were analysed with T1ρ mapping, T2 mapping and DHI. Furthermore, immunohistochemistry was performed with collagen type I, II and X staining and COX-2 staining.
Results: The DHI increased between T0-T6 after 1x NCM, 2x NCM and NCM+MSC treatment in the induced IVDs compared with the control IVD. A decreased T2 relaxation between T0-T6 is found after every treatment compared with the control group. No significant effects were found between T0-T6 with T1ρ mapping. Collagen type I and X are not deposited in the NPs of all the groups. Collagen type II is deposited in all groups and there are COX-2 positive cells detected in every group.
Conclusion: NCM reinjection improved the DHI and induced healthy ECM production. However, NCM treatment does not show a regenerative effect at quantitative T1ρ and T2 mapping. MSC treatment does not exert an additive effect.

Keywords: Intervertebral disc (IVD), degeneration, mesenchymal stromal cells (MSCs), notochordal cells (NCs), notochordal cell matrix (NCM), magnetic resonance imaging (MRI), T1ρ mapping, T2 mapping, disc height index (DHI).

Introduction

Healthy IVD

A healthy intervertebral disc (IVD) consists of a central nucleus pulposus (NP), a transition zone that is situated around the NP, an annulus fibrosus (AF) around the transition zone and cartilaginous endplates which are the cranial and caudal borders (figure 1) (Bergknut et al., 2013) . The transition zone is the zone where a fibrous structure becomes more cartilaginous (Bergknut et al., 2013). In a healthy IVD, the NP is hydrated and contains collagen type II and proteoglycans (PGs). There is a high osmotic pressure due to the fact that negatively charged PGs in the NP attract water and the swelling is restricted by the AF. The high osmotic pressure is needed to sustain compressive loads to maintain a healthy IVD. Also, notochordal cells (NCs) are present in the NP. These cells are only present in young human individuals and foetuses and are gradually replaced by chondrocyte-like nucleus pulposus cells (NPCs) during maturation (Bach et al., 2016).

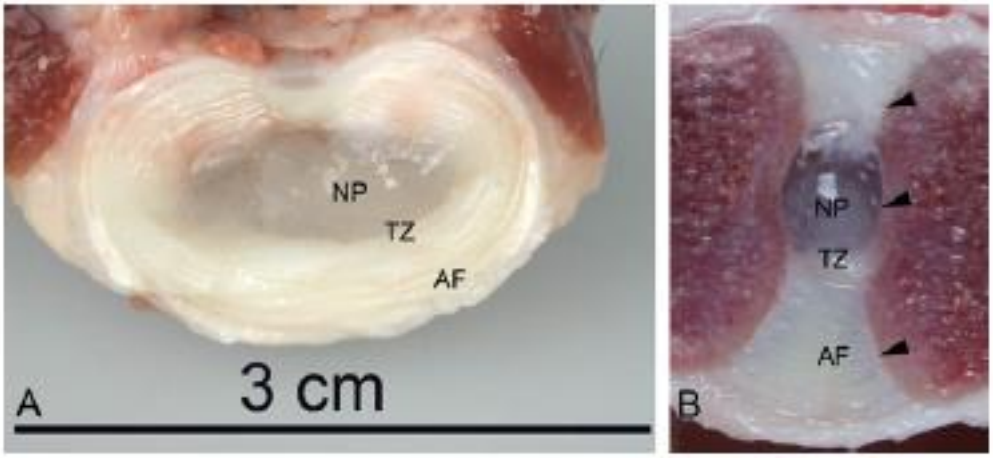

Figure 1. Healthy IVD wit A) transverse view and B) sagittal view. NP = nucleus pulposus, TZ = transition zone, AF = annulus fibrosus and the endplates are shown with the arrowheads (Bergknut et al., 2013).

Degeneration

Intervertebral disc (IVD) degeneration is a progressive condition, which is common in dogs and humans. During the degeneration process, the disc height decreases (Johannessen et al., 2006), a shift from collagen type II to collagen type I and a decrease in PG content is observed in the extracellular matrix of the NP and by this the tissue is less hydrated (Arkesteijn et al., 2015; Richardson et al., 2016; Willems et al., 2016). Besides, the notochordal cells (NCs) disappear and the population of apoptotic nucleus pulposus cells (NPCs) increase (Arkesteijn et al., 2015). Also, it is suggested that some inflammatory mediators, like prostaglandin E_2 (PGE_2), tumor necrosis factor α (TNF-α) and interleukins play a role in the catabolic process in NP and AF tissue (Willems et al., 2016). PGE_2 is synthesized by cyclooxygenase-1 and -2 (COX-1 and 2). COX-2 is believed to be important in the PGE_2 expression, which is produced in degenerative processes. Under physiological conditions, COX-2 is almost not produced, but it can be quickly expressed in response to inflammatory stimuli (Willems et al., 2016). A study of Willems *et al* it showed that PGE_2 levels and COX-2 expression is higher in degenerated canine IVDs compared to not degenerated IVDs (Willems et al., 2016) Not only inflammatory mediators may play a role, also fibrotic-like changes are seen whereby collagen type I is present (Yee et al., 2016). Also, hypertrophic differentiation is associated with degeneration and collagen type X seems to play a role here (Rutges, J P H J et al., 2010).

The most occurring symptom of IVD disease is low back pain (Bach et al., 2016; L. Smolders et al., 2013; Willems et al., 2016). In dogs, IVD degeneration can lead to cervical and thoracolumbar IVD herniation, degenerative lumbosacral stenosis and cervical spondylomyelopathy (Bergknut et al., 2011). IVD degeneration is more common in chondrodystrophic (CD) dog breeds than in non-chondrodystrophic breeds (NCD) and it develops around 3-7 years of age in CD breeds, while in NCD breeds it develops around 6-8 years of age (L. A. Smolders et al., 2013; Willems et al., 2016). In CD breeds it is characterized by a disturbed endochondral ossification of mostly the long bones and the Hansen type I is mostly seen in those breeds, while the Hansen type II is more seen in NCD breeds (Smolders et al., 2013; Willems et al., 2016).

To diagnose IVD disease, magnetic resonance imaging (MRI) and computed tomography (CT) are valuable diagnostics besides information on the medical history and physical and neurological examination (Bergknut et al., 2011; Kranenburg et al., 2013).
Magnetic resonance imaging is based on positively charged spinning hydrogen protons (H^+). These protons have individual magnetization vectors, which are orientated in the body and cancel out (Thrall, 2013). The energy that arises can be transferred by applying a radiofrequency pulse and is also called resonance. The protons jump to a higher state of energy because the energy is absorbed and causes a state of imbalance. When the protons stop spinning by stopping the radiofrequency pulse, the protons return to their original state, also called relaxation (Thrall, 2013). When relaxation starts, T1 and T2 processes occur and differ among tissues. The T1 relaxation is the time that is required for the longitudinal magnetization to recover, while the T2 relaxation is the time that is needed to eliminate the transverse net magnetization (Thrall, 2013). The MRI is believed to be the choice of imaging to detect advanced IVD degeneration, like changes in morphology, hydration, height and herniation (Johannessen et al., 2006), but it is not refined enough to detect early degeneration changes or type of herniation (Bergknut et al., 2011).
Since it made improvements over the last decade, new techniques like T1ρ and T2 mapping are used to expose early degenerative changes in the IVD in humans (Zhang et al., 2017).

T2 mapping gives information about the collagen, water content and orientation of matrix structure in cross-sectional studies as well as in longitudinal studies (Sun et al., 2013). The T2 values decreases with more degenerated IVDs and this suggests a decrease in PG and water content. Also, a down-regulation of collagen type II gene expression is found with decreased T2 values in the NP and this reflects the degradation and disorganisation of the collagen network in the degeneration process (Sun et al., 2013).
Not only the T2 mapping shows promising results, also T1ρ mapping shows this. It measures the relaxation time with a 'spin lock' pulse and it is sensitive to protons on macromolecules like glycosaminoglycan (GAG). An *in vitro* study of Johannessen *et al* found a correlation between the PG content in the NP and the T1ρ (Johannessen et al., 2006). The lower the water content, the lower the T1ρ values. Also, the more the IVD degenerates, the lower the T1ρ values are (Johannessen et al., 2006).
So, both T2 mapping and T1ρ mapping show potential and are non-invasive techniques to help diagnose IVD degeneration in earlier stages.
Next to this, it is possible to calculate the disc height index (DHI). This is the height of the IVD whereby the DHI decreases during degeneration (Hiyama et al., 2008; Johannessen et al., 2006; Serigano et al., 2010).

Current treatments for IVD disease, such as medication, physiotherapy or surgical treatment options like decompression with partial removal of the diseased IVD tissue, spinal fusion of the affected segment or artificial IVD replacement are symptom-oriented to relieve the pain, but do not repair the IVD itself (Smolders et al., 2013). The treatments that alleviate the pain are even associated with complications such as spinal instability, adjacent segment degeneration or failure of the surgical implants (Smolders et al., 2013). Therefore, the interest in regenerative treatments has increased.

Regenerative effects

Regenerative therapies that try to biologically repair of the degenerated IVD have gained interest over the past years and includes the use of growth factors, gene therapy and/or (stem) cells (Bach et al., 2014; Smolders et al., 2013). Because degeneration is related to a decrease of the cell population, cell therapy has potential to restore the IVD (de Vries et al., 2015; Sakai et al., 2006). Different cells, like mesenchymal stromal cells and notochordal cells may be able to achieve this by their capacities.

Mesenchymal stromal cells (MSCs)

Mesenchymal stromal cells (MSCs) are emerging as cellular therapy, because they can differentiate into other cell types and they support regenerative processes (Sakai et al., 2006; Smolders et al., 2013; Steffen, Smolders, Roentgen, Bertolo, & Stoyanov, 2017).
Previous work indicated that MSCs can restore the degenerated IVD (Arkesteijn et al., 2015; Hiyama et al., 2008; Richardson et al., 2016). MSCs are immature cells that remain pluripotent and depending on their environment they have multilineage potential (Hiyama et al., 2008; Serigano et al., 2010) They can differentiate toward a NPC-like phenotype after which they start producing PG or they can provide stimulatory effects on NPC proliferation and GAG production (Arkesteijn et al., 2015; de Vries et al., 2015; Ganey, Hutton, Moseley, Hedrick, & Meisel, 2009; Richardson et al., 2016). A combined stimulation of MSCs and NPCs show a better regenerative potential than MSCs alone (Arkesteijn et al., 2015; de Vries et al., 2015). An *in vitro* study showed an increased production of GAG with MSCs in coculture with notochordal cells and the majority of the MSCs disappeared during culture. However, only a minority differentiate towards chondrogenic phenotypes and thereby contributing to the matrix production (Arkesteijn et al., 2015).
An *in vivo* study with induced IVD degeneration and MSC transplantation in Beagles showed a delay in the progression of the disc degeneration with MSCs with a well-preserved inner annulus structure. Also, an increase of GAG was seen in comparison with the degenerated discs (Hiyama et al., 2008). Another *in vivo* study in dogs, similar to the study mentioned above, has shown that the collagen type II, GAG and other extracellular matrix components were maintained with MSCs, indicating that IVD degeneration is suppressed (Serigano et al., 2010).

Notochordal cells (NCs)

NCs that are located in the NP have restorative capacities. They exert a regenerative effect on other cells like mesenchymal stem cells (MSCs) and NPCs (Smolders et al., 2013). This is shown *in vitro* using a notochordal cell conditioned medium (NCCM), which induced glycosaminoglycan (GAG) and collagen type II deposition after 28 days in canine NPCs (Bach et al., 2016). Furthermore, anticatabolic effects on canine NPCs are shown as well, by a decrease of A desintegrin and metalloproteinase with thrombospondin motifs 5 (*ADAMTS5*) gene expression and matrix metalloproteinase 13 (*MMP13*), which are catabolic genes (de Vries et al., 2015). It is also shown *in vitro* that there is a cross-species effect of human,

canine and porcine NC-secreted factors on human NPCs derived from degenerated IVDs (Bach et al., 2016). Canine and porcine NCCM appears more potent than human NCCM, since they more potently increased NPC cell numbers and GAG deposition. However, only human NCCM induced collagen type II deposition which implies qualitative and quantitative differences in bioactive factors between human and porcine and canine NCCM (Bach et al., 2015).

There are soluble and pelletable factors present in NCCM, which consist of peptides and proteins (soluble) and protein aggregates and extracellular vesicles (pelletable). Mainly soluble NCCM (NCCM-S) factors showed anabolic effects on canine NPCs. In addition, notochord/nucleus pulposus specific marker expression was higher after treatment of NCCM-S and healthy NCCM (NCCM+) indicating a better way to induce healthy NP phenotype (Bach et al., 2016) . Next to this, more pericellular GAGs were found in NCCM-S and NCCM+, which suggests that NPCs produce the GAGs themselves (Bach et al., 2016). Not only canine NCCM+, but also porcine NCCM+ showed anabolic effects on canine NPCs, which shows a cross-species effect (Bach et al., 2016).
It is difficult to identify the NC secreted factors and thereby a new approach is being researched, namely notochordal cell matrix (NCM).

Notochordal cell matrix (NCM)

Direct use of the matrix of NP tissue rich in NCs, also called notochordal cell matrix (NCM) is a new approach as mentioned above. In previous in vitro work (not published yet), NCM was produced from healthy porcine NC-rich NP tissue by lyophilization and resuspension in basal culture medium (10 mg/mL). The effect of NCM was determined on canine and human NPCs derived from degenerated IVDs cultured in micro-aggregates for 28 days. NCM induced an anabolic, anti-catabolic, anti-apoptotic, and proliferative effect on human and canine NPCs derived from degenerated IVDs. Thus, directly applying notochordal cell matrix could be a promising regenerative treatment for canine and human IVD disease, circumventing the (challenging) identification and application of bioactive NC-secreted substances. Therefore, the long-term effects of NCM were thereafter determined in an experimental animal model *in vivo*.

Aim of the study

The goal of the complete study is to investigate if porcine NCM has regenerative effects on degenerated canine IVDs *in vivo* and if MSCs could exert an (additive) effect.
The specific aim of this sub study is to determine whether effects of NCM treatment are observed at MRI (T1ρ, T2 mapping, DHI) and protein expression level (collagen type I, II, X, COX-2).

Hypothesis

NCM treatment shows a regenerative effect at MRI (T1ρ, T2 mapping, DHI) and protein expression level (collagen type I, II and X) and MSC treatment can exert an additive effect.

Materials and methods

In vivo study with five Beagles

Five Beagles were used at the start of the experiment.
The effect of the different treatments, shown in figure 2, will be tested on early and more severely degenerated IVDs.
Six weeks before the start of the experiment (T = -1.5 months), severe IVD degeneration was induced in five IVDs per dog by nuclectomy (NX; T12-T13, L1-L2, L3-L4, L5-L6, and L7-S1). At the start of the experiment (T = 0 months), the early and severely degenerated canine IVDs were injected with 50 µL of (a) $1*10^6$ canine mesenchymal stromal cells (MSCs) incorporated in an albumin-based hydrogel (b) 10 mg/mL notochordal cell matrix (NCM), or (c) $1*10^6$ canine MSCs incorporated in 10 mg/mL NCM. Three months after the first injections (T = 3 months), two IVDs per dog (L6-L7 and L7-S1) were again injected with 50 µL of 10 mg/mL NCM. Every dog received a similar treatment per spinal location.

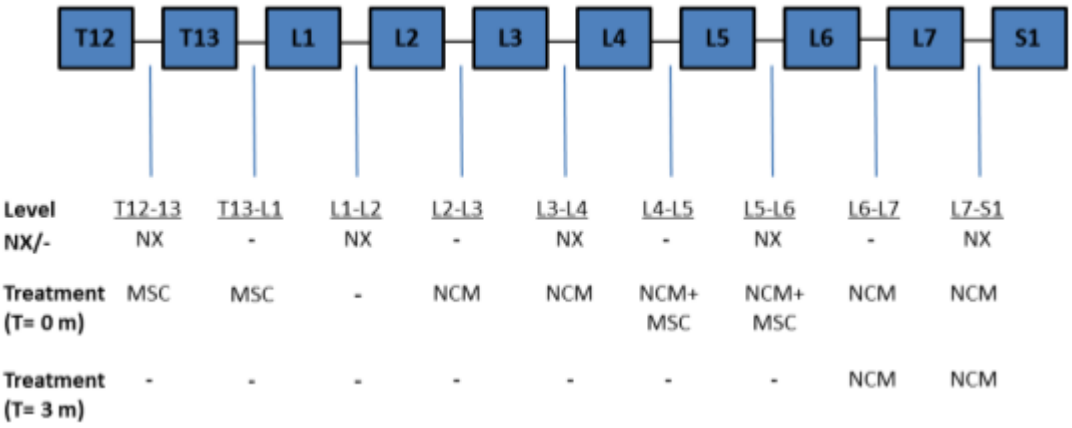

Figure 2. Intervertebral discs with induction (NX) and without induction (-) of degeneration and with different treatments with canine mesenchymal stromal cells (MSC), notochordal cell matrix (NCM), both MSC and NCM and no treatment. The vertebrae are numbered from T12 until S1.

MRI, DHI, T1ρ and T2 mapping

MRI

The MRI studies of the five beagles were performed at T=0, T=3 and T=6 months using a 1.5T high field MRI unit (Ingenia, Philips). The dogs were anesthetized by first using intravenous propofol (1-2 mg/kg) for induction and then anesthesia provided by intravenous dexmedetomidine (10 µg/kg) and butorphanol (0.2 mg/kg). Anaesthesia was maintained by inhalation isoflurane (1-1,5%). During MRI, the dogs were positioned in dorsal recumbency.
A sagittal T2-weighted Turbo Spin Echo sequence with repetition time of 3000 ms and echo time of 110 ms, was obtained by using a field of view (FOV) of 75x200 mm, acquisition matrix of and 124x261 and 13 slices with a thickness of slice 2 mm.
Sagittal T1ρ-weighted imaging was performed using a spinlock-prepared sequence with 3D multi-shot gradient echo (T1-TFE) readout with a FOV: of76 x 220 mm, an acquisition matrix of 76 x 220, a slice thickness of 2 mm, a TR/TE of 4.6s/2.3s, a TFE factor of 50, a flip angle of 45° and a shot interval of 3000 ms.

Data for the T1ρ was acquired by using spinlock times: 0, 10, 20, 30 and 40 ms with spinlock pulse amplitude of 500 Hz.
Data for T2 was acquired by using multiple sagittal spin-echo T2 mapping sequence with a FOV of 75x219 mm, acquisition time of 96x273, thickness of the slices of 3 mm, a repetition time of 200 ms and echos time of 13-104 ms (8 echoes were obtained with 13 ms echo spacing).

T1ρ and T2 values

An oval-shaped region of interest (ROI) was placed on the NP on the three mid-sagittal slices using Decay Analyses software. The mean T1ρ and T2 values within every ROI were calculated by using the Levenberg-Marquardt nonlinear least-squares method (Willems et al., 2015).

Disc height index (DHI)

The DHI was reviewed on mid-sagittal slices of T2W images on every IVD and calculation was done according to the method of Masuda *et al*, see also figure 3 (Masuda et al., 2006). To calculate the DHI of T11-T12 and L7-S1, the average body height of T12 was used for T11 and the average body height of L7 was used for S1 because T11 and S1 were not present on all MRI's. The MRI's for the DHI were reviewed in DICOM viewer Horos for Mac.

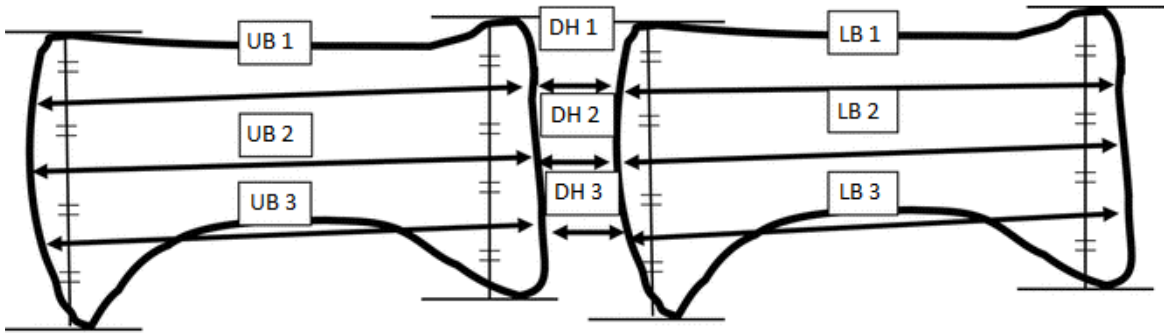

$$DHI = \frac{2(DH1 + DH2 + DH3)}{(LB1 + LB2 + LB3) + (UB1 + UB2 + UB3)}$$

Figure 3. UB = upper body, LB = lower body, DH = disc height. The DHI is expressed in percentages (Masuda et al., 2006).

Immunohistochemistry for collagen I, II and X and COX-2

Collagen I and II

For collagen type I and II, the slides were deparaffinised in xylene (2 times 5 minutes) and then hydrated with 96% ethanol 5 minutes, 80% ethanol 5 minutes, 70% ethanol 5 minutes and 60% ethanol 5 minutes. The slides were washed in PBS for 5 minutes and then incubated with 0.3% H_2O_2 for 10 minutes at room temperature. The slides were then washed with PBS-T 0.1% for 2 times 5 minutes and rounds were made with PAP-pen around the tissue. Antigen retrieval with pronase (1 mg/ml) was done for 30 minutes at 37°C. The slides were washed

again in PBS-T 0.1% for 2 times 5 minutes and then antigen retrieval with hyaluronidase (10 mg/ml) was done for 30 minutes at 37ºC. After this, the slides were washed another time with PBS-T 0.1% for 2 times 5 minutes and then the slides were incubated over night with primary antibody for collagen I (1 ab6308 Mouse monoclonal antibody 100µg/mL, IgG1, dilution 1:1500) and collagen II (mouse monoclonal antibody DSHB, II-II6B3 42µg/mL, dilution 1:2000, IgG1) at 4ºC. The negative control was incubated over night with normal mouse IgG1 Santa Cruz sc3877, 50µg/mL, dilution 1:750 at 4ºC.

The next day, the slides were washed with PBS-T 0.1% (2 times, 5 minutes) and incubated with secondary antibody conjugated HRP EnVision+ System-HRP Goat Anti-Mouse at room temperature for 60 minutes. After incubation, the slides were washed with PBS (2 times, 5 minutes) and incubated in DAB peroxidase substrate solution for 1 minute. The slides were rinsed in MQ and after this they were rinsed in demi water. Counterstaining with Hematoxylin QS-Solution was done for 1 minute. Thereafter, the slides were rinsed in running tap water for 10 minutes. The slides were then dehydrated through 60% ethanol (5 minutes), 70% ethanol (5 minutes), 80% ethanol (5 minutes), 96% ethanol (2 times, 5 minutes), 100% ethanol (5 minutes) and cleared in xylene (2 times, 5 minutes). The slides were mounted with Depex.

Collagen X

For collagen X staining, we stained 50 samples and 5 negative controls. The slides were deparaffinised as described for collagen I and II. The slides were washed in PBS for 5 minutes and PBS-T 0.1% for 5 minutes. The tissue was circled by the PAP-pen and antigen retrieval with 0.1% pepsin was done for 20 minutes at 37ºC. The slides were washed in PBS-T 0.1% (2 times 5 minutes) and then antigen retrieval with hyaluronidase 10mg/ml was done for 30 minutes at 37ºC. The slides were washed in PBS-T 0.1% (2 times 5 minutes) and the block with DAKO dual endogenous enzyme was done for 5 minutes. The slides were rinsed one time with PBS and incubated afterwards with PBS for 5 minutes. The slides were incubated with the dilution of normal goat serum 1:10 in PBS-T 0.1% (80µL/tissue) for 30 minutes at room temperature. Afterwards the slides were incubated overnight with primary antibody collagen X mouse monoclonal (400 µg/mL, dilution 1:50 PBS/BSA 5%, IgG1, 80µL/tissue). The 5 negative controls were incubated overnight with normal mouse IgG1 (50µg/mL, dilution 1:20.000 in PBS/BSA 5%, 80µL/tissue).

The next day the slides were washed with PBS-T 0.1% for 2 times 5 minutes. Then they were incubated with Secondary Antibody conjugated with HRP (EnVision+ system-HRP Anti-Mouse) for 30 minutes at room temperature. The slides were then washed with PBS for 2 times 5 minutes and incubated in DAB peroxidase substrate solution for 1 minute. The slides were rinsed in MQ briefly and rinsed in demi water briefly. The counterstaining with Hematoxylin QS solution was done for 1 minute and afterwards the slides were rinsed in running tap water for 10 minutes. Dehydration was done through 70% ethanol for 5 minutes, 80% ethanol for 5 minutes, 95% ethanol for 2 times 5 minutes, 100% ethanol for 5 minutes and cleared in xylene for 2 times 5 minutes. The slides were mounted with Depex.

COX-2

For COX-2, we stained 50 samples and 1 negative control. The slides were deparaffinised as described for collagen I and II. The slides were washed in MQ for 5 minutes and the tissue was circled by the PAP-pen. The tissue was blocked with Endogenous enzyme block (Dako, S2003) for 10 minutes at room temperature and then the slides were washed in TBS-T 0.1% (2 times, 5 minutes). The tissue was blocked with TBS-BSA 5% for 60 minutes at room

temperature and then the slides were incubated overnight with primary antibody monoclonal antibody IgG1 (Clone CX229, 400 µg/mL, EDTA dilution 1:50 in TBS/BSA 5%, 78 µL/tissue). The negative control was incubated overnight with normal mouse IgG1 Santa Cruz (sc3877, 50µg/mL, EDTA dilution 1:20 in TBS/BSA 5%, 78 µL/tissue).

The next day the slides were washed with TBS-T 0.1% (2 times, 5 minutes) and incubated with secondary antibody conjugated with HRP (EnVision+ system-HRP Anti-Mouse) at room temperature for 30 minutes. The slides were then washed in TBS (2 times 5 minutes) and then incubated in DAB peroxidase substrate solution for 5 minutes. The slides were washed in MQ (2 times 5 minutes) to stop DAB reaction. The counterstaining with Hematoxylin QS solution was done for 1 minute and afterwards the slides were rinsed in running tap water for 10 minutes. Dehydration was done as described for collagen type X and at last the slides were mounted with Depex.

Statistics

For the DHI, T1ρ and T2 mapping the cox proportioned hazard model (coxph) was used with the donors as a random effect.
Statistical significance was considered at p-value ≤ 0.05 and further evaluated with use of the effect sizes (ES). Non-parametric ES were calculated and provided as *Cliff's delta*. To describe them, the rules developed by Vargha *et al.* were used: *small* if $ES<0.28$, *medium* if $0.28\leq ES<0.43$, *large* if $0.43\leq ES<0.7$, very *large* if $0.7\leq ES<1$ (Vargha, 2000). As threshold for this study, small ES were considered as uncertain, independently of its p-value; if $p\leq 0.05$, medium and larger ES, if $0.05<p\leq 0.1$, large and larger ES, and if $0.1<p\leq 0.15$ very large and very large ES, were considered as relevant or as substantive significant (Ellis, 2012; Greenland et al., 2016).
The intraclass correlation coefficient was calculated in IBM SPSS Statistics version 24 for Mac.

Results

MRI

The intraclass correlation coefficient for the T1ρ and T2 mapping was excellent (0.957 and 0.980, respectively).

DHI of IVDs that were not induced

The DHI was significantly increased after MSC treatment compared with the control group at T=0 and T=3 months ($p \leq 0.05$ and $p \leq 0.15$ with a large or very large effect size, figure 4A-B).
The MSC treatment also significantly increased the DHI at T=0 ($p \leq 0.01$), T=3 ($p \leq 0.15$ with a large or very large effect size) and T=6 ($p \leq 0.05$) compared with the NCM+MSC treatment (figure 4A-C).
The DHI of the 2x NCM treatment significantly increased compared with NCM+MSC treatment and T=3 and T=6 ($p \leq 0.15$ with large or very large effect size and $p \leq 0.05$, figure 4B-C).
The DHI of the control group did not significantly differ from the other treatment groups at T=3 and T=6 (figure 4B-C).
The 2x NCM-treated IVDs showed a significantly increased DHI delta between T0-T6 compared with the control group and MSC treatment group ($p \leq 0.15$ with large or very large effect size, figure 4D). The 2x NCM treatment increased the DHI with 3,5%, while the MSC treatment decreased the DHI with 1%.
The DHI delta between T0-T3 did not show significantly differences between groups (figure 4E).
The NCM+MSC- and 2x NCM-treated IVDs showed a significantly decreased DHI delta between T3-T6 compared with the control group ($p \leq 0.01$ and $p \leq 0.05$, figure 4F). The MSC-treated IVDs showed a significant increased DHI delta between T3-T6 compared with 1x NCM ($p \leq 0.15$ with large or very large effect size), 2x NCM ($p \leq 0.01$) and NCM+MSC ($p \leq 0.01$) treatments (figure 4F).

DHI of the control and induced IVDs

The 1x NCM-treated IVDs and NCM+MSC treated-IVDs showed a significantly decreased DHI at T=0 compared to the control group ($p \leq 0.05$ and $p \leq 0.01$, figure 4A). The 2x NCM-treated IVDs however, showed a significantly increased DHI at T=0 compared to the control group ($p \leq 0.05$, figure 4A).
The DHI of the induced IVDs without treatment was significantly increased at T=0 compared with the 1x NCM-treated IVDs ($p \leq 0.01$) and the NCM+MSC treatment ($p \leq 0.001$), but significantly decreased at T=0 and T=3 compared with 2x NCM ($p \leq 0.15$ with large or very large effect size, figure 4A-B).
The NCM+MSC treatment decreased the DHI at T=0 and T=3 compared with the 2x NCM treatment and MSC treatment ($p \leq 0.001$ at T=0 and $p \leq 0.001$ and $p \leq 0.01$ at T=3, figure 4A-B).
The DHI significantly increased at T=3 after 2x NCM treatment ($p \leq 0.01$) and MSC treatment ($p \leq 0.15$ with large or very large effect size) compared to the control group (figure 4B)
The induced IVDs without treatment showed a significantly increased DHI at T=3 compared with the NCM+MSC treatment group ($p \leq 0.01$, figure 4B).
The 2x NCM-treated IVDs showed a significantly increased DHI at T=6 compared with all other groups except the MSC treatment (control group $p \leq 0.05$, no treatment group and 1x NCM treatment ($p \leq 0.15$ with large or very large effect size) and NCM+MSC treatment ($p \leq 0.01$, figure 4C). The NCM+MSC-treated IVDs showed a significantly decreased DHI at

T=6 compared with all the groups except the control group (no treatment group and 1x NCM treatment ($p \leq 0.15$ with large or very large effect size), 2x NCM treatment ($p \leq 0.01$) and MSC treatment ($p \leq 0.05$, figure 4C).
The DHI delta between T0-T6 significantly increased after 1x NCM, 2x NCM and NCM+MSC treatment ($p \leq 0.15$ with large or very large effect size,) compared with the control IVDs and the no treatment group (figure 4D).
The DHI delta between T0-T3 did not show significantly differences in all groups (figure 4E).
Between T3-T6 the DHI was significantly increased after 1x NCM, 2x NCM and NCM+MSC treatment compared with the control group ($p \leq 0.05$, figure 4F). Also, between T3-T6 the DHI was significantly decreased after MSC treatment compared with the control group ($p \leq 0.05$, figure 4F).
The DHI delta between T3-T6 of the no treatment group significantly decreased compared with 1x NCM ($p \leq 0.15$ with large or very large effect size), MSC ($p \leq 0.15$ with large or very large effect size) and NCM+MSC treatment ($p \leq 0.05$, figure 4F).

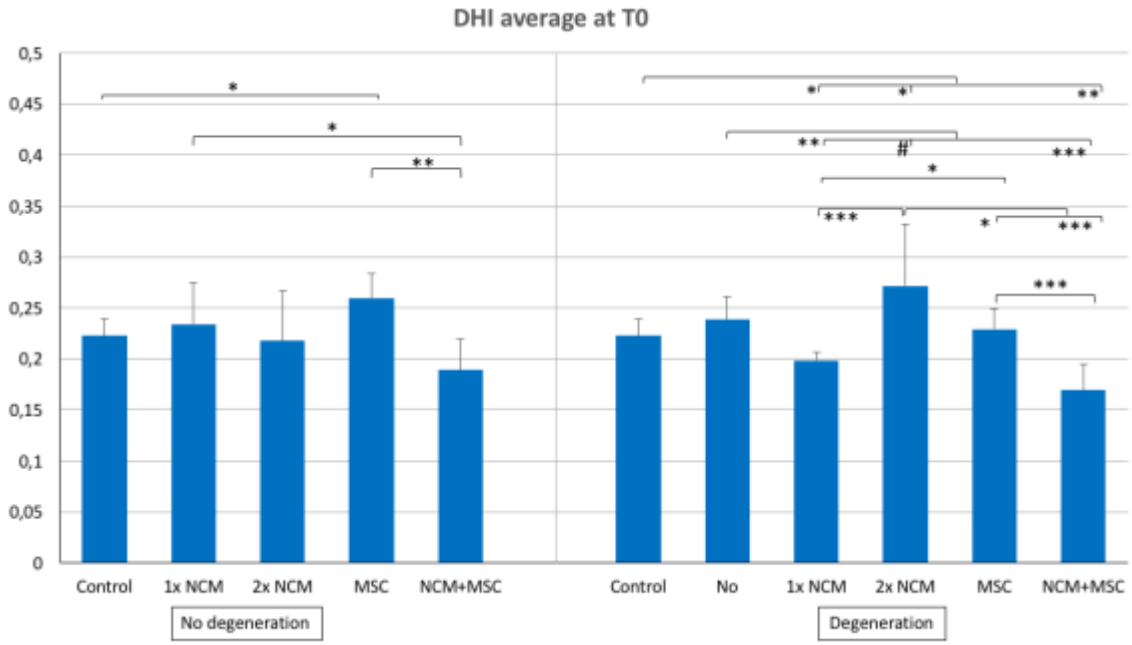

Figure 4A. Disc height index (DHI) average results of all donors at T=0 months. Control = control IVDs without induction; no treatment = induced IVDs without treatment; 1x NCM = treatment with notochordal cell matrix (NCM) at T=0; 2x NCM = treatment with notochordal cell matrix at T=0 and T=3; MSC = treatment with mesenchymal stromal cells (MSC) at T=0; NCM+MSC = treatment with notochordal cell matrix and mesenchymal stromal cell at T=0. The left bars in the graph are the not-induced IVDs and the bars on the right in the graph are the induced IVDs. # = $p < 0.15$, with large or very large effect size (ES); * = $p < 0.05$; ** = $p < 0.01$; *** = $p < 0.001$ N=5

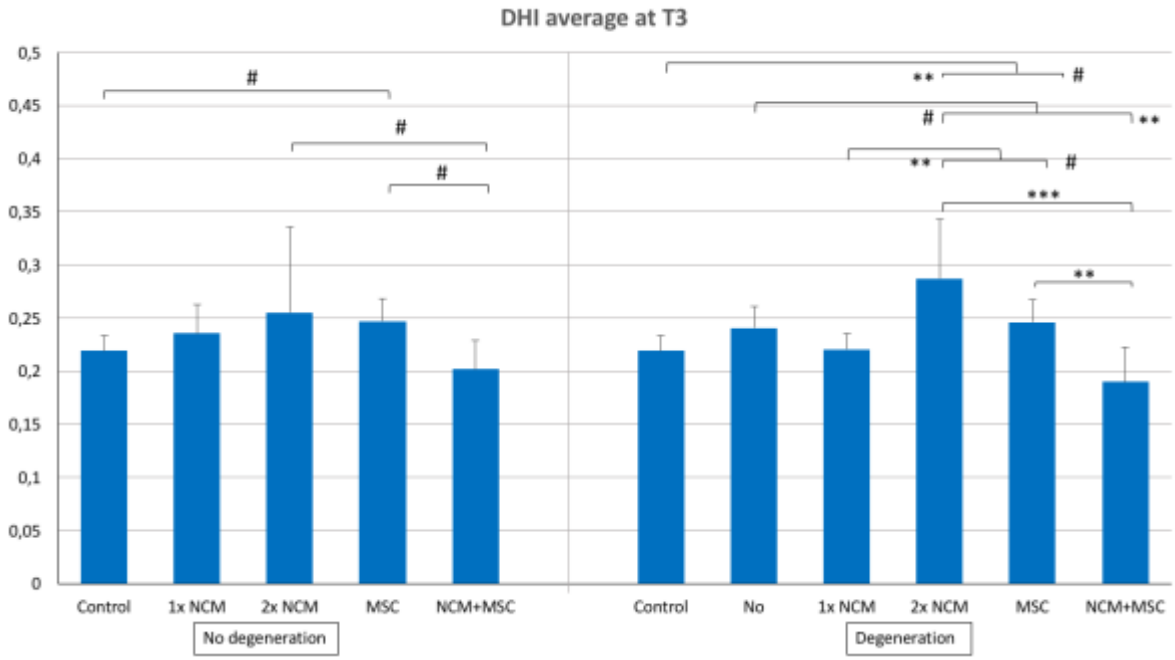

Figure 4B. DHI average results of all donors at T=3 months. Control = control IVDs without induction; no treatment = induced IVDs without treatment; 1x NCM = treatment with notochordal cell matrix (NCM) at T=0; 2x NCM = treatment with notochordal cell matrix at T=0 and T=3; MSC = treatment with mesenchymal stromal cells (MSC) at T=0; NCM+MSC = treatment with notochordal cell matrix and mesenchymal stromal cell at T=0. The left bars in the graph are the not-induced IVDs and the bars on the right in the graph are the induced IVDs. # = $p < 0.15$, but large or very large ES; ** = $p < 0.01$; *** = $p < 0.001$. N=5

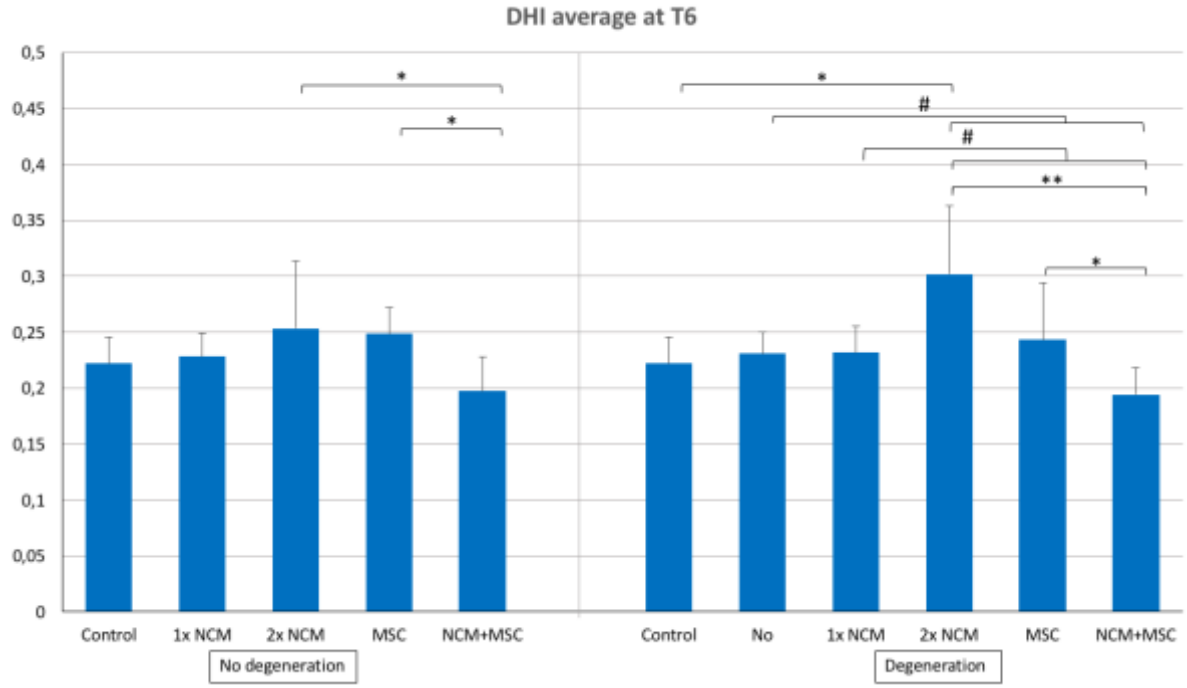

Figure 4C. DHI average results of all donors at T=6 months. Control = control IVDs without induction; no treatment = induced IVDs without treatment; 1x NCM = treatment with notochordal cell matrix (NCM) at T=0; 2x NCM = treatment with notochordal cell matrix at T=0 and T=3; MSC = treatment with mesenchymal stromal cells (MSC) at T=0; NCM+MSC = treatment with notochordal cell matrix and mesenchymal stromal cell at T=0. The left bars in the graph are the not-induced IVDs and the bars on the right in the graph are the induced IVDs. # = $p < 0.15$, but large or very large ES; * = $p < 0.05$; ** = $p < 0.01$. N=5

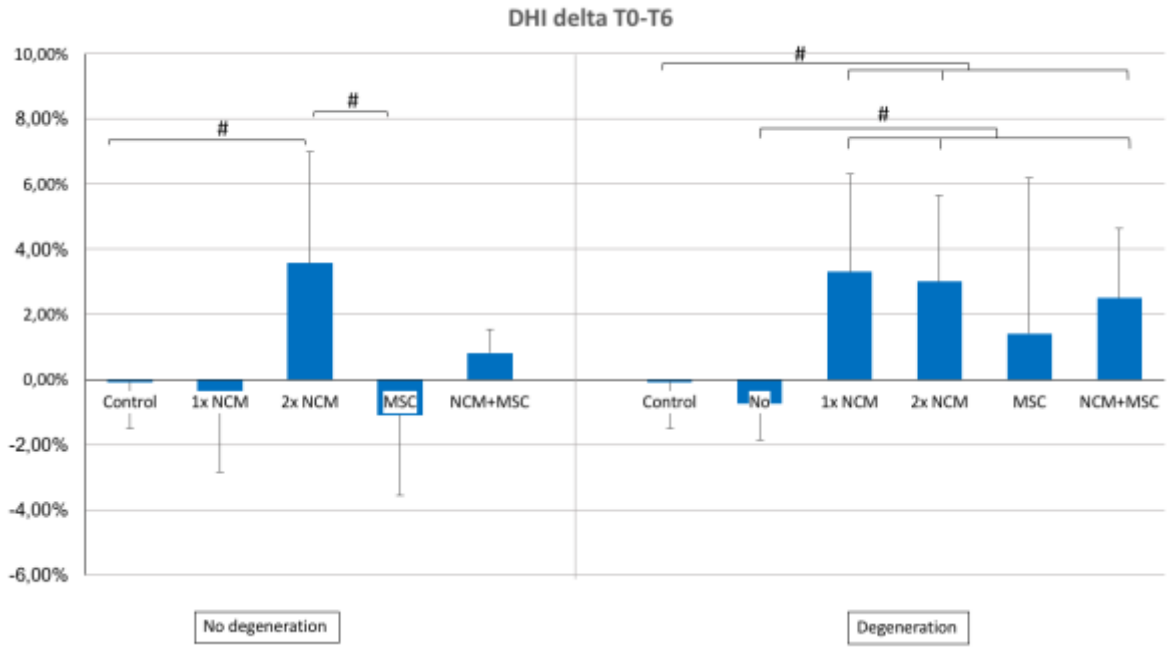

Figure 4D. DHI delta between T0 and T6. The percentages per treatment shown here are the results of the DHI at T=6 months – the DHI at T=0 months. Control = control IVDs without induction; no treatment = induced IVDs without treatment; 1x NCM = treatment with notochordal cell matrix (NCM) at T=0; 2x NCM = treatment with notochordal cell matrix at T=0 and T=3; MSC = treatment with mesenchymal stromal cells (MSC) at T=0; NCM+MSC = treatment with notochordal cell matrix and mesenchymal stromal cell at T=0. The left bars in the graph are the not-induced IVDs and the bars on the right in the graph are the induced IVDs. # = $p < 0.15$, but large or very large ES. N=5

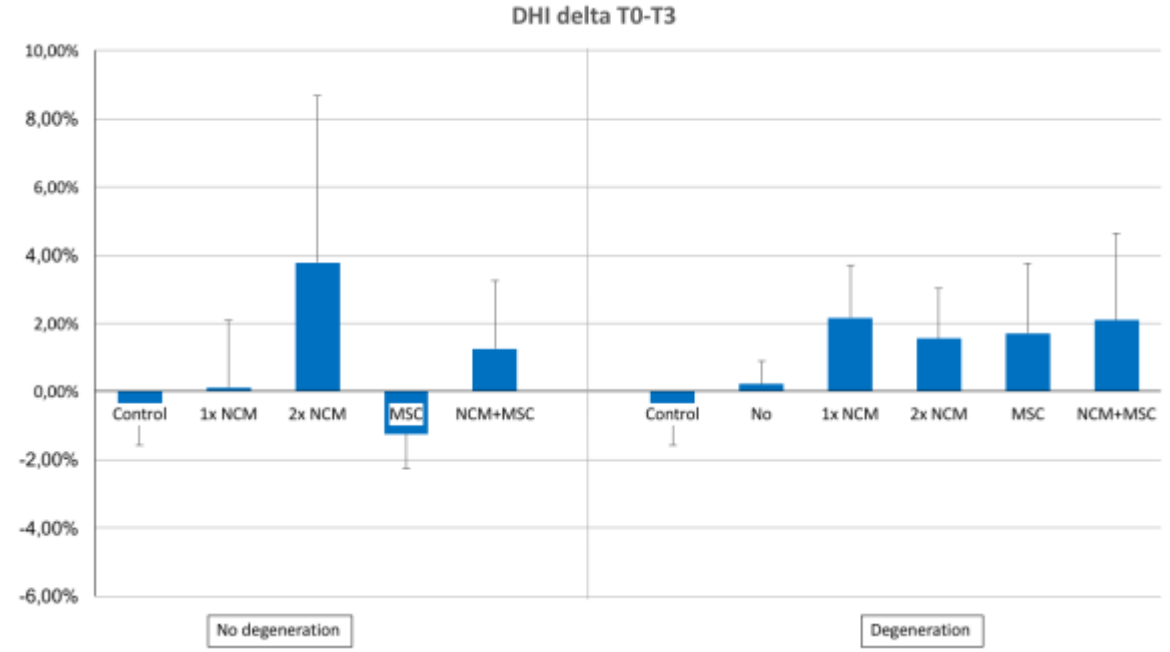

Figure 4E. DHI delta between T0 and T3. The percentages per treatment shown here are the results of the DHI at T=3 months – the DHI at T=0 months. Control = control IVDs without induction; no treatment = induced IVDs without treatment; 1x NCM = treatment with notochordal cell matrix (NCM) at T=0; 2x NCM = treatment with notochordal cell matrix at T=0 and T=3; MSC = treatment with mesenchymal stromal cells (MSC) at T=0; NCM+MSC = treatment with notochordal cell matrix and mesenchymal stromal cell at T=0. The left bars in the graph are the not-induced IVDs and the bars on the right in the graph are the induced IVDs. The groups did not show significantly differences in DHI. N=5

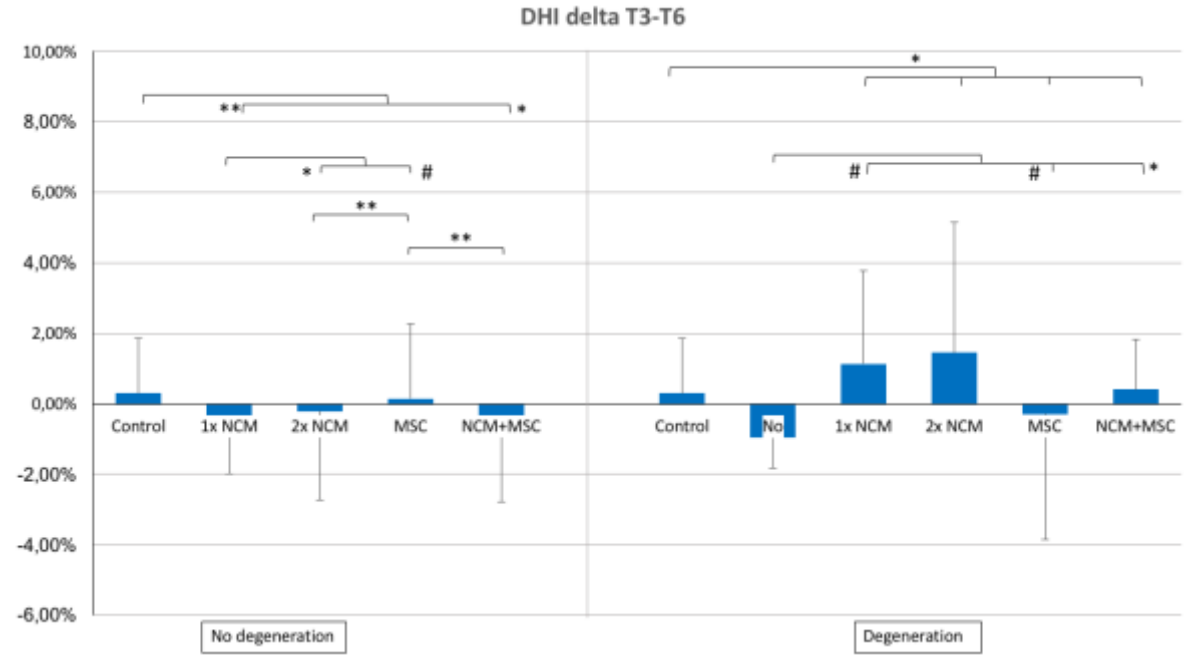

Figure 4F. DHI delta between T3 and T6. The percentages per treatment shown here are the results of the HI at T=6 months – the DHI at T=3 months. Control = control IVDs without induction; no treatment = induced IVDs without treatment; 1x NCM = treatment with notochordal cell matrix (NCM) at T=0; 2x NCM = treatment with notochordal cell matrix at T=0 and T=3; MSC = treatment with mesenchymal stromal cells (MSC) at T=0; NCM+MSC = treatment with notochordal cell matrix and mesenchymal stromal cell at T=0. The left bars in the graph are the not-induced IVDs and the bars on the right in the graph are the induced IVDs. # = $p < 0.15$, but large or very large ES; * = $p < 0.05$; ** = $p < 0.01$. N=5

T2 mapping of the IVDs that were not induced

The quantitative T2 mapping did not show significantly differences between treatments at T=0, T=3 and T=6. Quantitative T2 mapping delta between T0-T6, T0-T3 and T3-T6 did not show significantly differences between the groups.

T2 mapping of the control and induced IVDs

The not-treated IVDs ($p \leq 0.05$), 1x NCM ($p \leq 0.01$) and MSC treatment ($p \leq 0.05$) at T=0 showed a significantly decreased quantitative T2 mapping compared with the control group (figure 5A). The 2x NCM treatment group showed a significantly increased quantitative T2 mapping compared with the 1x NCM treatment at T=0 ($p \leq 0.05$, figure 5A).
The quantitative T2 mapping was significantly decreased at T=3 and T=6 after the not-treated IVDs ($p \leq 0.05$), 1x NCM ($p \leq 0.001$), 2x NCM ($p \leq 0.05$), MSC ($p \leq 0.05$) and NCM+MSC treatment ($p \leq 0.05$) compared with the control group (figure 5B-C).
The quantitative T2 mapping was significantly decreased after 1x NCM treatment at T=3 and T=6 compared with 2x NCM ($p \leq 0.05$ and $p \leq 0.01$), MSC ($p \leq 0,05$) and NCM+MSC treatment ($p \leq 0.05$, figure 5B-C). The no treatment group showed a significantly increased quantitative T2 mapping at T=6 compared with 1x NCM treatment ($p \leq 0.05$, figure 5C).
The not-treated IVDs ($p \leq 0.15$, with large or very large effect size), 1x NCM ($p \leq 0.01$ and $p \leq 0.05$), 2x NCM ($p \leq 0.05$), MSC ($p \leq 0.15$, with large or very large effect size and $p \leq 0.05$) and NCM+MSC treatment ($p \leq 0.15$, with large or very large effect size and $p \leq 0.05$) showed a significantly decreased quantitative T2 mapping delta between T0-T6 and T0-T3 compared with the control group (figure 5D-E).

The not-treated IVDs showed a significantly increased quantitative T2 mapping delta between T0-T6 compared with 1x NCM treatment (p≤0.15, with large or very large effect size, figure 5D).
The quantitative T2 mapping delta between T3-T6 of the 1x NCM was significantly decreased compared with the control group and 2x NCM treatment (p≤0.15, with large or very large effect size, figure 5F).

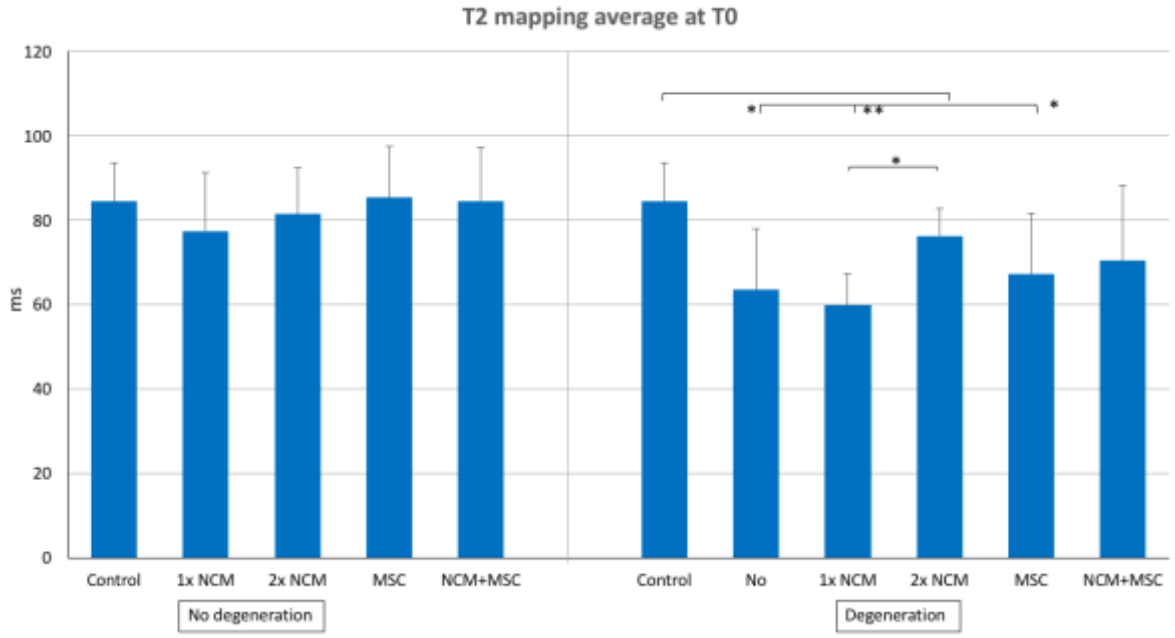

Figure 5A. T2 mapping average results of all donors at T=0 months. Control = control IVDs without induction; no treatment = induced IVDs without treatment; 1x NCM = treatment with notochordal cell matrix (NCM) at T=0; 2x NCM = treatment with notochordal cell matrix at T=0 and T=3; MSC = treatment with mesenchymal stromal cells (MSC) at T=0; NCM+MSC = treatment with notochordal cell matrix and mesenchymal stromal cell at T=0. The left bars in the graph are the not-induced IVDs and the bars on the right in the graph are the induced IVDs. * = $p < 0.05$; ** = $p < 0.01$. N=5

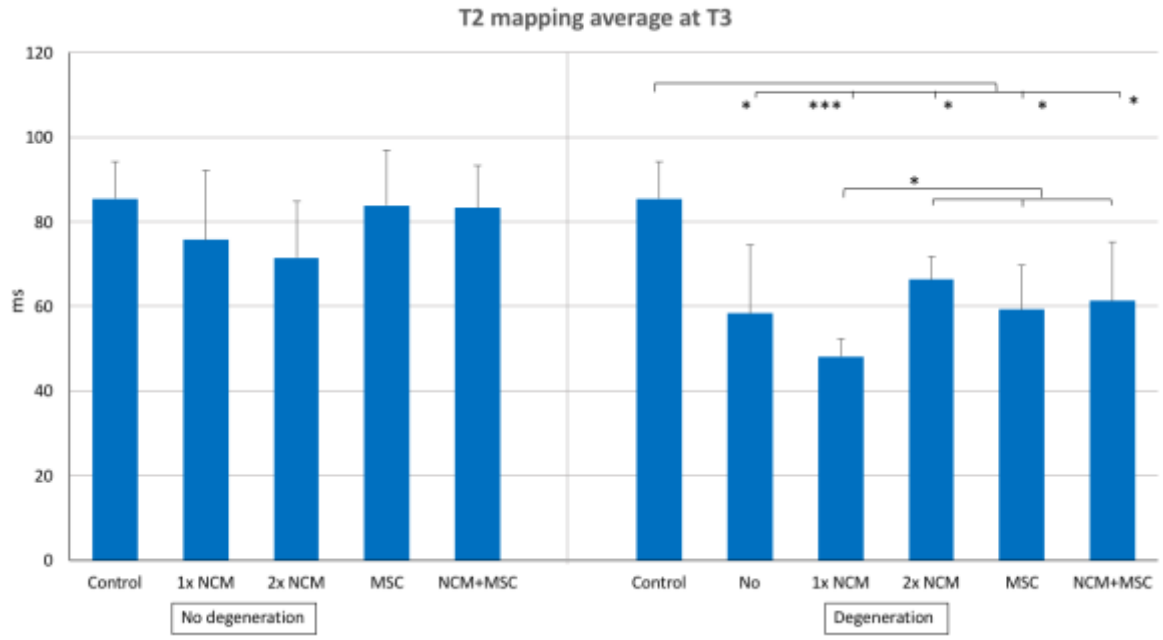

Figure 5B. T2 mapping average results of all donors at T=3 months. Control = control IVDs without induction; no treatment = induced IVDs without treatment; 1x NCM = treatment with notochordal cell matrix (NCM) at T=0; 2x NCM = treatment with notochordal cell matrix at T=0 and T=3; MSC = treatment with mesenchymal stromal cells (MSC) at T=0; NCM+MSC = treatment with notochordal cell matrix and mesenchymal stromal cell at T=0. The left bars in the graph are the not-induced IVDs and the bars on the right in the graph are the induced IVDs. * = $p < 0.05$; *** = $p < 0.001$. N=5

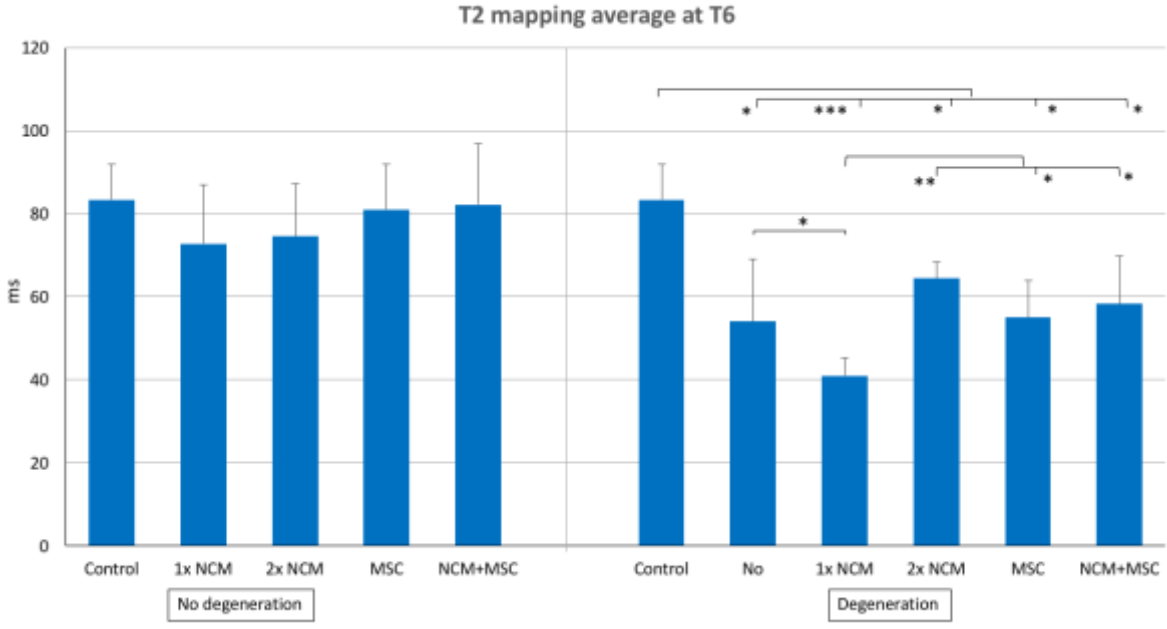

Figure 5C. T2 mapping average results of all donors at T=6 months. Control = control IVDs without induction; no treatment = induced IVDs without treatment; 1x NCM = treatment with notochordal cell matrix (NCM) at T=0; 2x NCM = treatment with notochordal cell matrix at T=0 and T=3; MSC = treatment with mesenchymal stromal cells (MSC) at T=0; NCM+MSC = treatment with notochordal cell matrix and mesenchymal stromal cell at T=0. The left bars in the graph are the not-induced IVDs and the bars on the right in the graph are the induced IVDs. * = $p < 0.05$; ** = $p < 0.01$; *** = $p < 0.001$. N=5

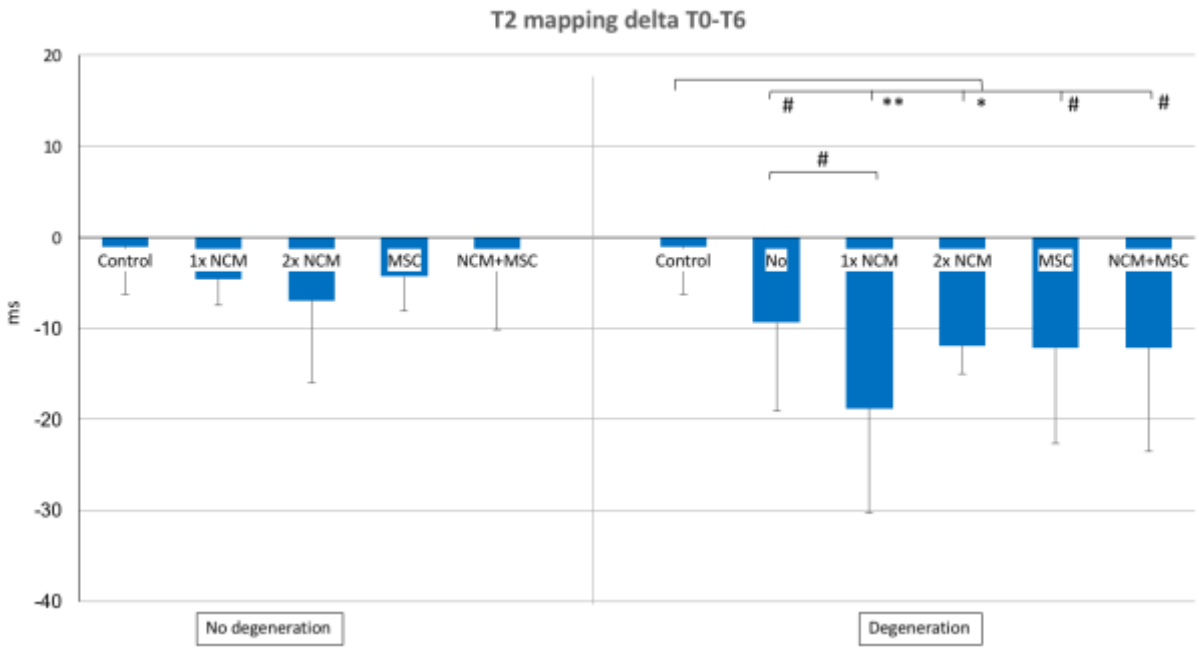

Figure 5D. T2 mapping results delta between T0 and T6. Control = control IVDs without induction; no treatment = induced IVDs without treatment; 1x NCM = treatment with notochordal cell matrix (NCM) at T=0; 2x NCM = treatment with notochordal cell matrix at T=0 and T=3; MSC = treatment with mesenchymal stromal cells (MSC) at T=0; NCM+MSC = treatment with notochordal cell matrix and mesenchymal stromal cell at T=0. The left bars in the graph are the not-induced IVDs and the bars on the right in the graph are the induced IVDs. # = $p < 0.15$, but large or very large ES; * = $p < 0.05$; ** = $p < 0.01$. N=5

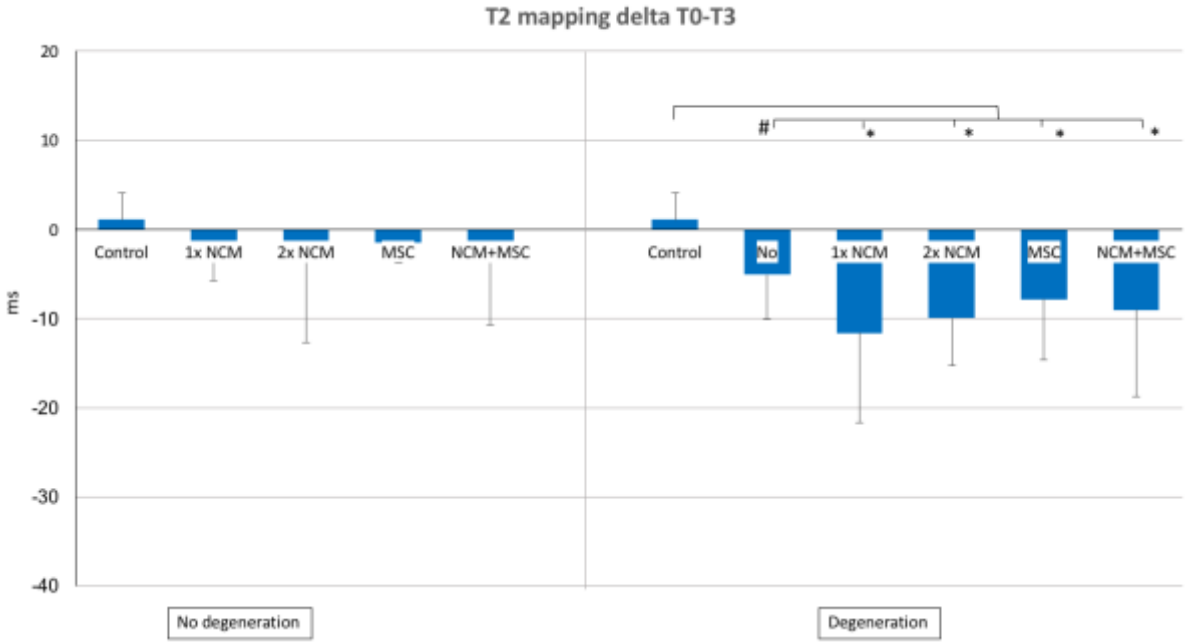

Figure 5E. T2 mapping results delta between T0 and T3. Control = control IVDs without induction; no treatment = induced IVDs without treatment; 1x NCM = treatment with notochordal cell matrix (NCM) at T=0; 2x NCM = treatment with notochordal cell matrix at T=0 and T=3; MSC = treatment with mesenchymal stromal cells (MSC) at T=0; NCM+MSC = treatment with notochordal cell matrix and mesenchymal stromal cell at T=0. The left bars in the graph are the not-induced IVDs and the bars on the right in the graph are the induced IVDs. # = $p < 0.15$, but large or very large ES; * = $p < 0.05$. N=5

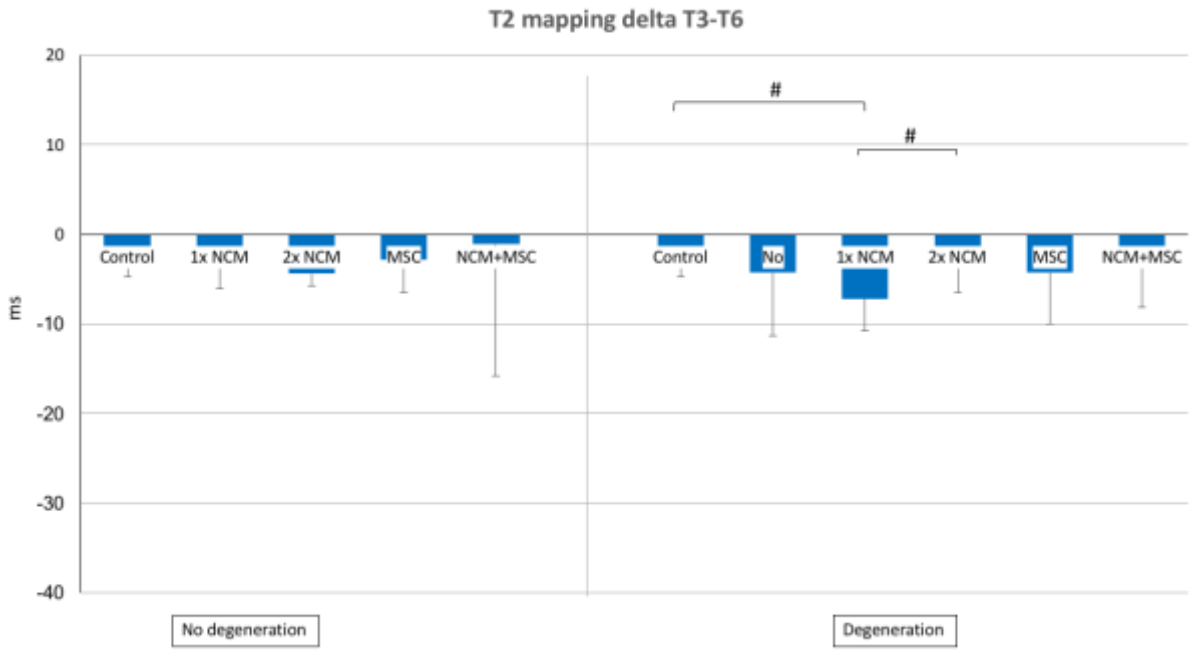

Figure 5F. T2 mapping results delta between T3 and T6. Control = control IVDs without induction; no treatment = induced IVDs without treatment; 1x NCM = treatment with notochordal cell matrix (NCM) at T=0; 2x NCM = treatment with notochordal cell matrix at T=0 and T=3; MSC = treatment with mesenchymal stromal cells (MSC) at T=0; NCM+MSC = treatment with notochordal cell matrix and mesenchymal stromal cell at T=0. The left bars in the graph are the not-induced IVDs and the bars on the right in the graph are the induced IVDs, # = $p < 0.15$, but large or very large ES. N=5

T1ρ mapping of the IVDs that were not induced

The T1ρ mapping did not show significantly differences at T=0, T=3 and T=6 (figure 6A-C). The T1ρ mapping delta between T0-T6, T0-T3 and T3-T6 did not show significantly differences between the groups.

T1ρ mapping of the control and induced IVDs

The not-treated IVDs ($p \leq 0.01$), 1x NCM ($p \leq 0.01$), 2x NCM ($p \leq 0.05$), MSC ($p \leq 0.01$) and NCM+MSC treatment ($p \leq 0.05$) showed a significantly increased T1ρ relaxation time compared with the control group figure 6A).
The T1ρ relaxation was significantly decreased after 1x NCM treatment ($p \leq 0.05$) at T=3 compared with the control group (figure 6B).
The not-treated IVDs ($p \leq 0.15$, with large or very large effect size), 1x NCM ($p \leq 0.01$), 2x NCM ($p \leq 0.05$) and MSC treatment ($p \leq 0.05$, figure 5C). The T1ρ mapping after 1x NCM treatment significantly decreased at T=6 compared with the no treatment group ($p \leq 0.15$, with large or very large effect size) and NCM+MSC treatment ($p \leq 0.05$) showed a significantly decreased T1ρ relaxation time at T=6 compared with the control group (figure 5C).
The T1ρ mapping delta between T0-T6 (figure 6D), T0-T3 and T3-T6 did not show significantly differences between the groups.

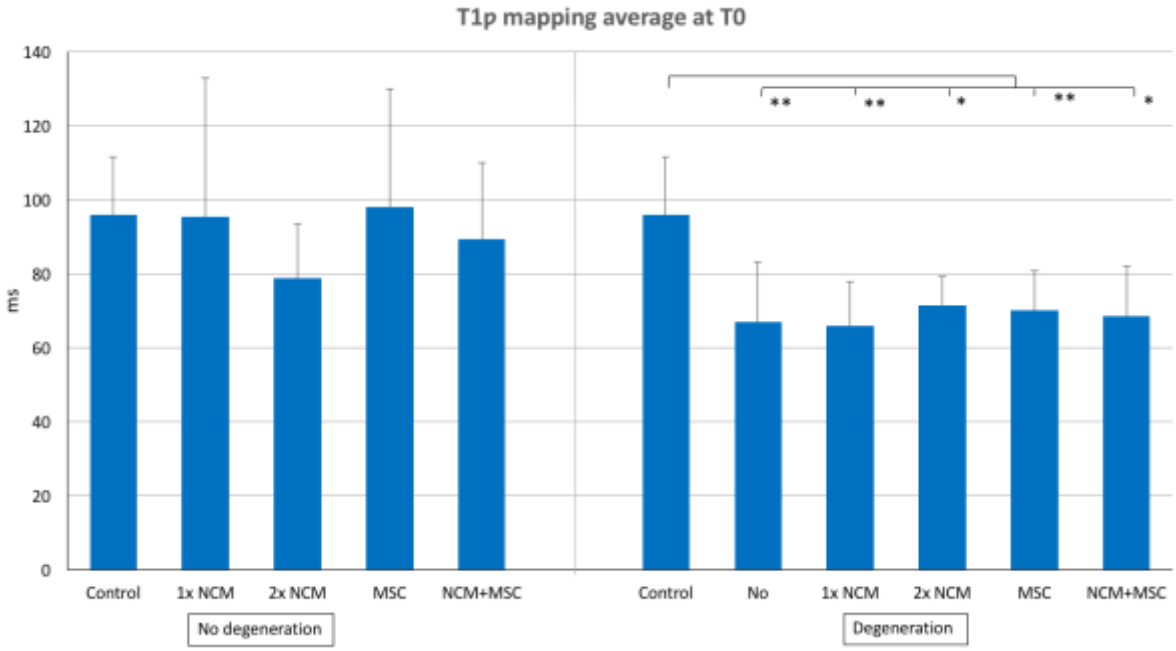

Figure 6A. T1ρ mapping average results of all donors at T=0 months. Control = control IVDs without induction; no treatment = induced IVDs without treatment; 1x NCM = treatment with notochordal cell matrix (NCM) at T=0; 2x NCM = treatment with notochordal cell matrix at T=0 and T=3; MSC = treatment with mesenchymal stromal cells (MSC) at T=0; NCM+MSC = treatment with notochordal cell matrix and mesenchymal stromal cell at T=0. The left bars in the graph are the not-induced IVDs and the bars on the right in the graph are the induced IVDs. * = $p < 0.05$; ** = $p < 0.01$. N=5

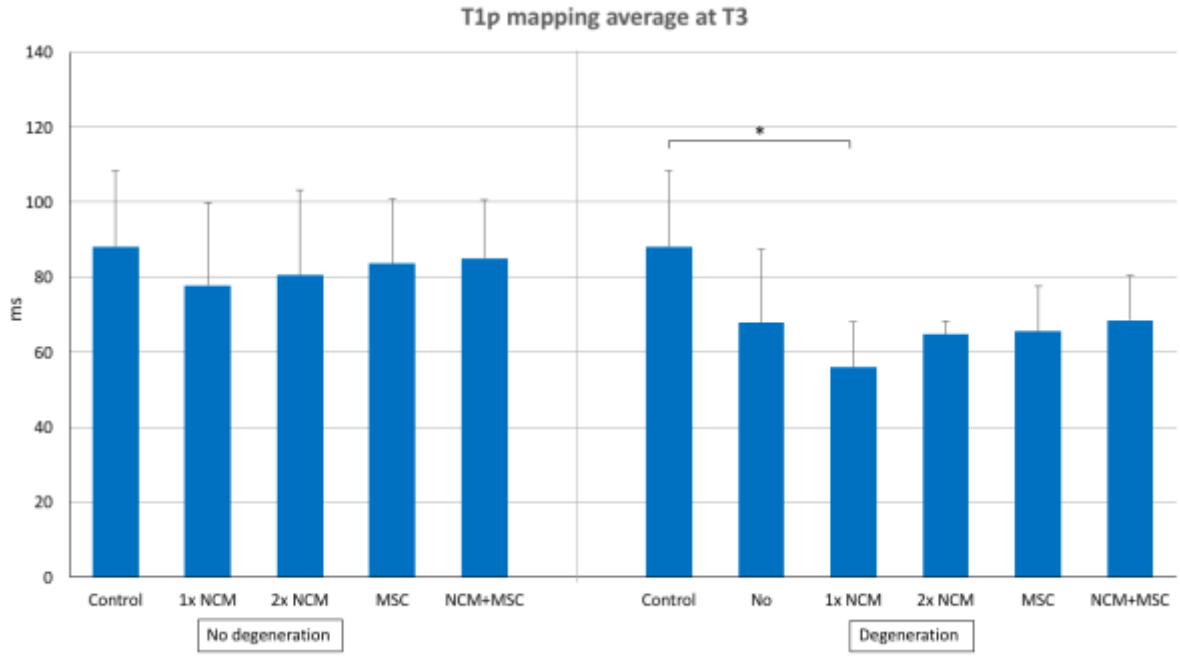

Figure 6B. T1ρ mapping average results of all donors at T=3 months. Control = control IVDs without induction; no treatment = induced IVDs without treatment; 1x NCM = treatment with notochordal cell matrix (NCM) at T=0; 2x NCM = treatment with notochordal cell matrix at T=0 and T=3; MSC = treatment with mesenchymal stromal cells (MSC) at T=0; NCM+MSC = treatment with notochordal cell matrix and mesenchymal stromal cell at T=0. The left bars in the graph are the not-induced IVDs and the bars on the right in the graph are the induced IVDs. * = $p < 0.05$. N=5

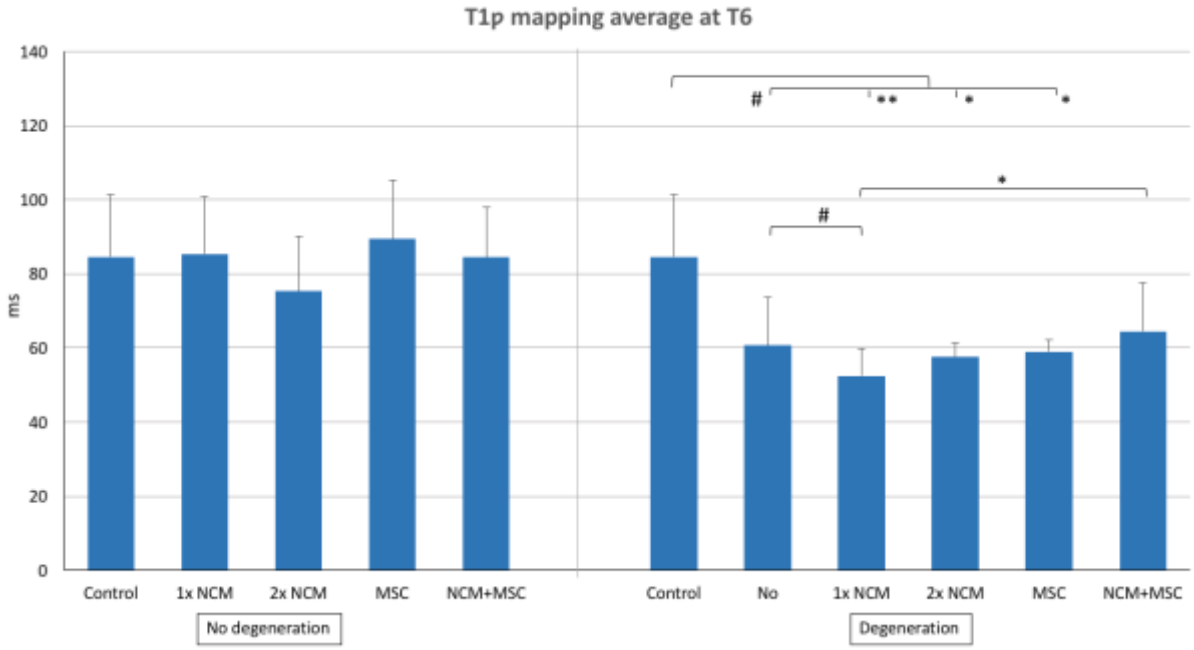

Figure 6C. T1ρ mapping average results of all donors at T=6 months. Control = control IVDs without induction; no treatment = induced IVDs without treatment; 1x NCM = treatment with notochordal cell matrix (NCM) at T=0; 2x NCM = treatment with notochordal cell matrix at T=0 and T=3; MSC = treatment with mesenchymal stromal cells (MSC) at T=0; NCM+MSC = treatment with notochordal cell matrix and mesenchymal stromal cell at T=0. The left bars in the graph are the not-induced IVDs and the bars on the right in the graph are the induced IVDs. # = $p < 0.15$, but large or very large ES; * = $p < 0.05$; ** = $p < 0.01$. N=5

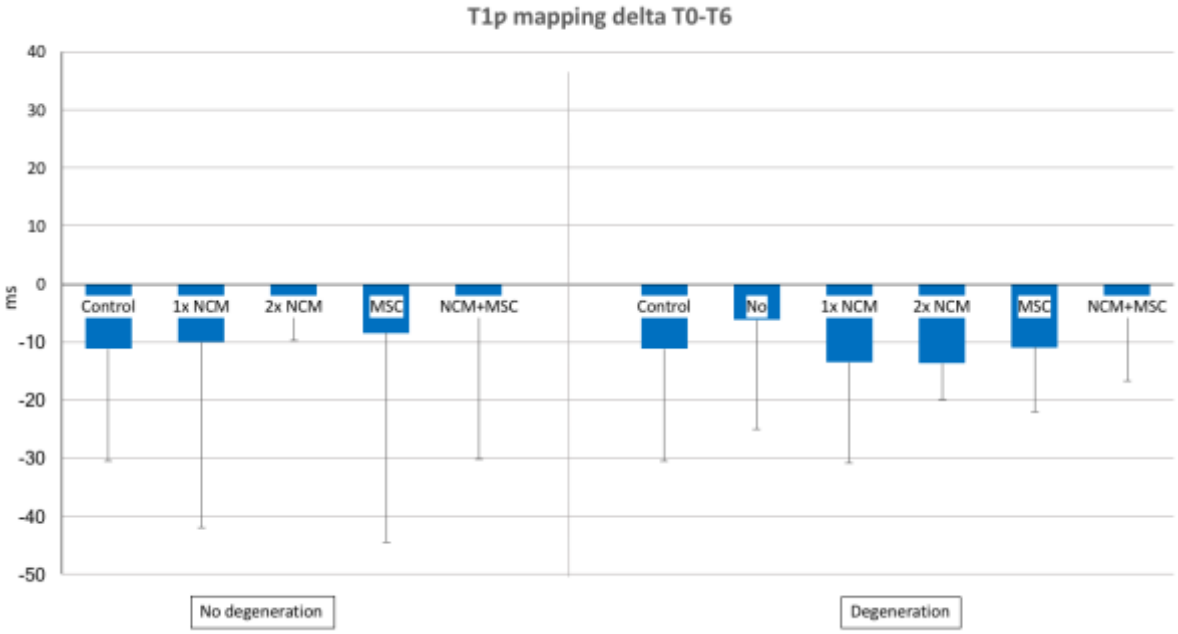

Figure 6D. T1ρ mapping average results of all donors between T=0 and T=6 months. Control = control IVDs without induction; no treatment = induced IVDs without treatment; 1x NCM = treatment with notochordal cell matrix (NCM) at T=0; 2x NCM = treatment with notochordal cell matrix at T=0 and T=3; MSC = treatment with mesenchymal stromal cells (MSC) at T=0; NCM+MSC = treatment with notochordal cell matrix and mesenchymal stromal cell at T=0. The left bars in the graph are the not-induced IVDs and the bars on the right in the graph are the induced IVDs. No significant differences were found. N = 5

Immunohistochemistry

Collagen type I is not present in the NP of both the control IVD and the induced IVD without treatment (figure 7).
Collagen type II is present in all groups (figure 8). The control group has the highest collagen type II deposition, while the MSC treatment group shows the least collagen type II deposition followed by the no treatment group. 2xNCM induced collagen deposition compared with the no treatment IVDs.
Collagen type X is not detected in both the control and the induced IVD without treatment (figure 7).
The COX-2 staining shows positive COX-2 cells in all treatment groups (figure 9), with no differences between conditions.

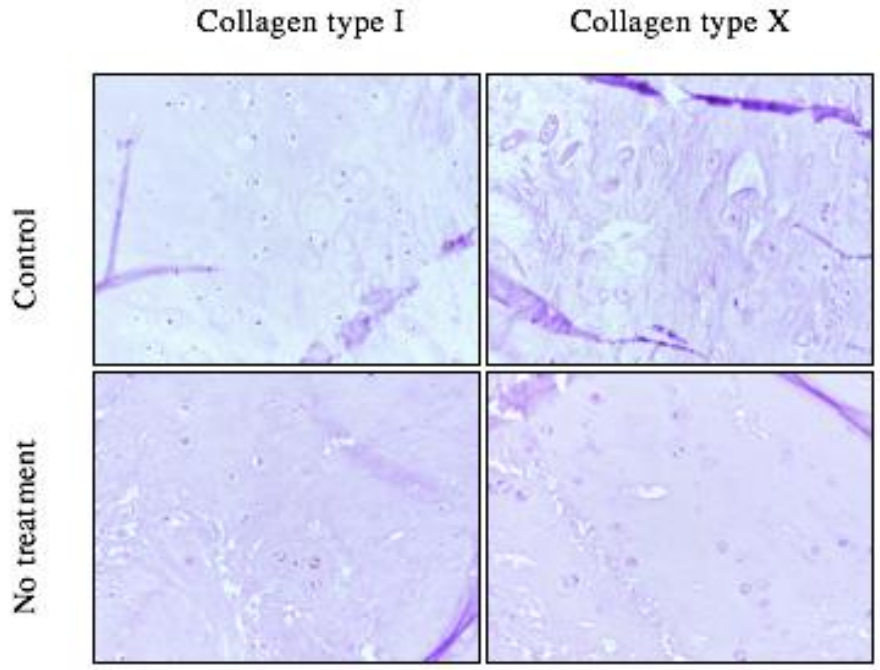

Figure 7. Pictures of the nucleus pulposus (NP) of the intervertebral discs (IVDs) with collagen type I, II and X and COX-2 staining. Control = control IVDs without induction; no treatment = induced IVDs without treatment. Collagen type I is not present in the control IVD but is present in the induced IVD without treatment. The collagen type II is present in both IVDs, but is more deposited in the control IVD than the induced IVD without treatment. Collagen type X is not present in both IVDs.

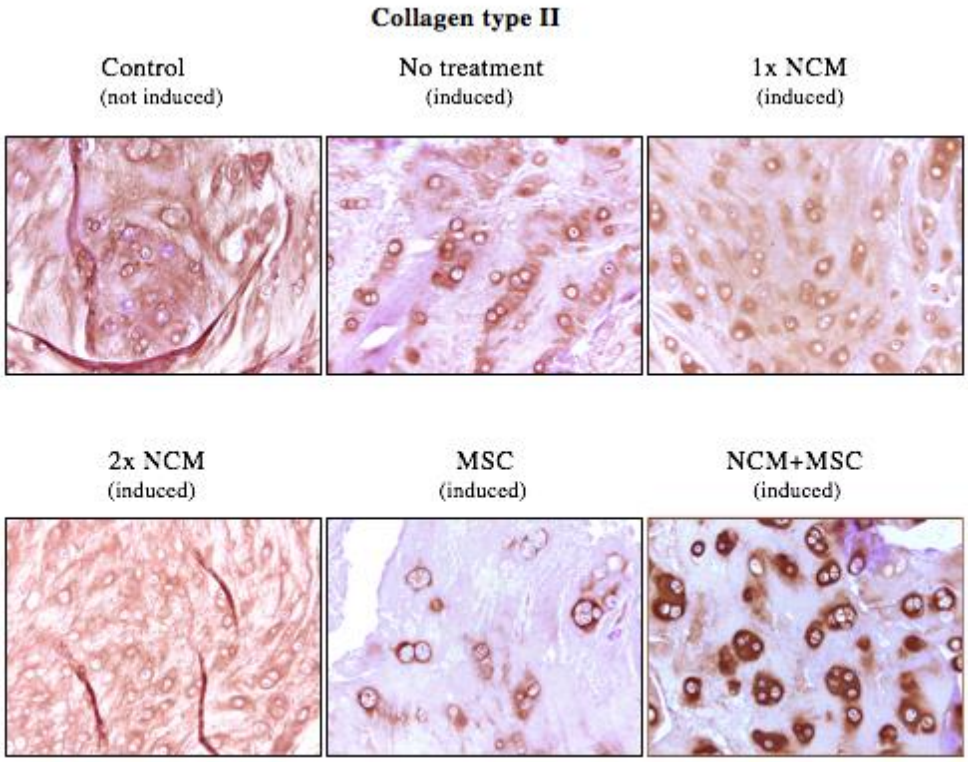

Figure 8. Pictures of the NP of the control IVD and of the induced IVDs with different treatments with collagen type II staining. Control = control IVDs without induction; no treatment = induced IVDs without treatment; 1x NCM = treatment with notochordal cell matrix (NCM) at T=0; 2x NCM = treatment with notochordal cell matrix at T=0 and T=3; MSC = treatment with mesenchymal stromal cells (MSC) at T=0; NCM+MSC = treatment with notochordal cell matrix and mesenchymal stromal cell at T=0. Collagen type II is present in all IVDs, but is more deposited in the control group, 1x NCM and 2x NCM treatment group than the induced group without treatment and the groups with MSC treatment and NCM+MSC treatment.

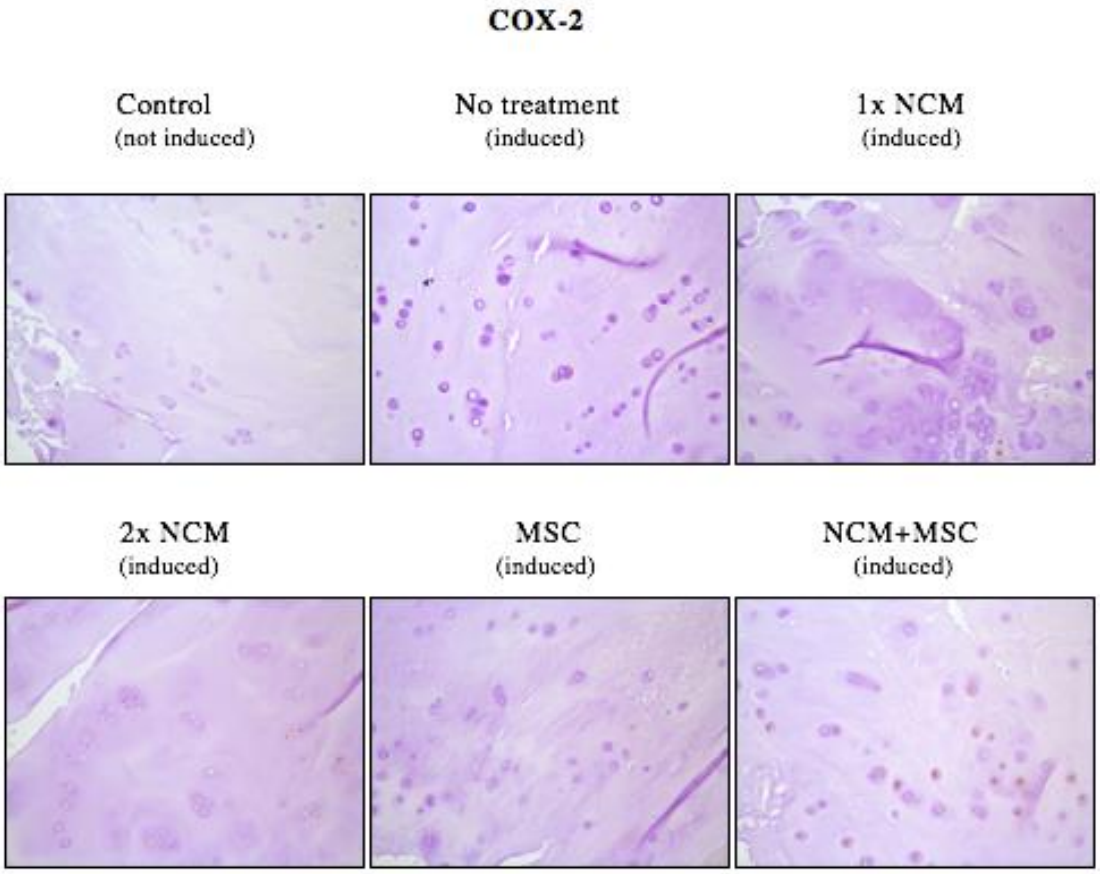

Figure 8. Pictures of the NP of the control IVD and of the induced IVDs with different treatments with collagen type II staining. Control = control IVDs without induction; no treatment = induced IVDs without treatment; 1x NCM = treatment with notochordal cell matrix (NCM; 2x NCM = treatment with notochordal cell matrix; MSC = treatment with mesenchymal stromal cells (MSC); NCM+MSC = treatment with notochordal cell matrix and mesenchymal stromal cell. COX-2 positive cells are seen in all treatment groups,

Discussion

Degeneration of the IVD is related to a decrease of cells and cell therapy has the potential to restore the IVD. Mesenchymal stromal cells (MSCs) and notochordal cells (NCs) have the potential to achieve regeneration because both cell types have shown to stimulate the GAG production and proliferation of NPCs. Because it is difficult to identify the NC secreted factors the whole notochordal cell matrix (NCM) is being used. The regenerative effects of NCM is seen on human and canine NPCs *in vitro* and now the long-term effects are determined in an *in vivo* study.

The aim of this study was to determine whether effects of NCM treatment are observed at MRI (T1ρ, T2 mapping, DHI) and protein expression level (collagen type I, II, X and COX-2) and if MSC treatment can exert an additive effect.
To our knowledge, this is the first study using NCM in induced and non-induced IVDs of canines *in vivo*. This is a longitudinal study, where the treatments were analysed using relatively new MRI techniques and immunohistochemistry.

MRI and immunohistochemistry

Disc height index

In our study, we did not find a decreased DHI of the induced, not-treated IVDs compared to the control group over a period of six months (figure 4D). This is in contrast with the findings of Serigano *et al*, where they did find a significant decreased DHI of induced IVDs compared to the control group (Serigano et al., 2010). A reason for the findings in our study could be because we started measuring after six weeks of induction and not directly after the moment of induction. It could be possible that the DHI is improved in these first six weeks. However, another possibility is that our sample size is too low in comparison with the study of Serigano *et al* where they used 30 Beagles (Serigano et al., 2010).

Secondly, we found that the DHI of the 2x NCM treatment group without induction was significantly increased compared to the control and MSC treatment group without induction between T=0 and T=6. The reason for an increased DHI after 2x NCM treatment could be because of the injected volume or because of the treatment itself.
The other treatments did not give an increased DHI over a period of six months with the same injected volume, but the 2x NCM treatment was given twice and so we cannot exclude that the injected volume could still play a role. However, it is not plausible that the injected volume is the cause for the increased DHI in six months, because the volume is absorbed within a few hours and is not present anymore after six months. Also, when looking at the results between the T=3 and T=6 we detected a decreased DHI after 2x NCM treatment in not-induced IVDs compared to the control group. This means that the increased DHI after 2x NCM treatment between T=0 and T=6 was already established during the first three months and is not influenced by the second injection, suggesting that the treatment itself resulted in an increased DHI thus had a positive effect on not-induced IVDs (figure 4D-F).
Furthermore, in the IVDs in which NX was performed, the 2x NCM treatment induced an increased DHI between T=0 and T=6 compared with the not-treated IVDs and the MSC+ control-treated IVDs. This suggests a regenerative effect on DHI after 2x NCM treatment in induced IVDs.

Thirdly, when looking at the induced IVDs over a period of six months, it is noticed that the 1x NCM and NCM+MSC treatments had a significantly increased DHI compared to the control group and the not-treated IVDs (figure 4D). Because the 1x NCM and NCM+MSC treatments did not give an increased DHI in the not-induced IVDs, we can hypothesize that the injection itself is not a reason for the increased DHI in the induced IVDs. This suggests that 1x NCM and NCM+MSC treatments have a positive effect on induced IVDs.

Lastly, we did not find a regenerative effect of induced IVDs after MSC treatment between T=0 and T=6 months compared with induced not-treated IVDs (figure 4D). This not consistent with the findings of Serigano *et al* and Hiyama *et al* where they found an increased DHI of induced IVDs after MSC treatment compared with the induced not-treated IVDs (Hiyama et al., 2008; Serigano et al., 2010). This increase was found in the first 16 respectively 12 weeks after induction. Also, in a study of Sakai *et al*, where they used rabbits, they found a significant increase of the DHI 10 weeks after MSC treatment in induced IVDs compared to the control group (Sakai et al., 2006). A reason why we did not find a significant increase in DHI after MSC treatment could be due to the fact that we used allogenic MSCs and the above-mentioned studies used autologous MSCs. However, in a study of Steffen *et al* and Ganey *et al* they used also autologous MSCs in degenerated IVDs of canines and they did not find a significant increase of the DHI after this treatment compared to the control IVDs (Ganey et al., 2009; Steffen et al., 2017). This is consistent with our findings, although we used allogenic MSCs. Another reason for the different results between the studies could be due to the fact that MSCs are a heterogenous population and the effects of the MSCs can differ between donor and also within the donor itself (Phinney, 2012) .

Quantitative T2 mapping

We found a decreased T2 mapping at T=0, T=3 and T=6 months and between T=0 and T=6 period in induced, not-treated IVDs compared to the control IVDs. This is consistent with studies of Sun *et al* and Zhang *et al*, where quantitative T2 mapping decreased in the NP during degeneration (Sun et al., 2013; Zhang et al., 2017). These findings suggest that T2 mapping can be used successfully to diagnose IVD degeneration.

Additionally, we found a decreased T2 relaxation time at T=3, T=6 and between T=0 and T=6 in the induced IVDs with 1x NCM, 2x NCM, MSC and NCM+MSC treatments compared to the control group (figure 5B-D), suggesting a degenerative effect in the IVDs despite the different treatments given. The reason why we did not find an increase in T2 relaxation time could be because MSCs did not exert a regenerative effect in our study. We did find collagen type II staining in the induced IVDs after MSC treatments, but this was not as high as the other treatment groups. This too suggests that MSC treatment does not exert a regenerative effect in our study. The other treatments also gave a decreased T2 mapping and is not consistent with our findings with collagen type II IHC. We detected collagen type II immunopositivity in all treatment groups, but most abundant in the 2x NCM treatment group. As mentioned earlier the T2 relaxation time is influenced by the collagen type II (17) and a reason for the inconsistent findings in our study could be due to the fact that diagnostic imaging is not as sensitive as histology (Serigano et al., 2010), that the treatments interfered with the orientation of the matrix or that T2 mapping could not detect regeneration of the IVD, but these theories cannot be supported with literature.

Furthermore, when looking at the results of the not induced IVD treatment groups no significant results were found, suggesting that there is no effect in and between the groups. This could mean that the treatments do not have an effect on non-degenerated IVDs.

Quantitative T1ρ

In our study, we found a decreased T1ρ relaxation time at T=0 months of the induced not-treated IVDs, but also in the induced IVDs after 1x NCM, 2x NCM, MSC and NCM+MSC treatments compared with the control group. This shows that the induction of the IVDs are measurable with T1ρ mapping. This is consistent with the findings of Zhang *et al* where they found decreased T1ρ relaxation times in degenerated IVDs (Zhang et al., 2017).
Also, we found at T=6 months the induced not-treated IVDs shows a decreased T1ρ relaxation time compared to the control group, suggesting that degeneration of the IVD is still detectable after six months.

Secondly, there were no significant effects between T=0 and T=6 after any treatment compared to the control group, suggesting that there is no effect of the treatments on the induced IVDs.
A reason why we did not find any effects could be due to the fact that the MRI is not sensitive enough to detect the effects. Another reason is that there is no effect. To see whether the MRI is not sensitive enough, it is important to compare quantitative biochemical data, like GAG content in the NP, with the results of the MRI.
To our knowledge, this is the first study using T1ρ mapping to detect changes in IVDs after cellular therapy.

ECM deposition

Lastly, we did not detect collagen type I and X in the NPs of the different treatment groups. This is in line with a study of Bach *et al* (2016), where no collagen type I was detected in the NPs after NCCM treatment (Bach et al., 2016). In another study of Bach *et al* (2015) there was no collagen type X found in the NPs (Bach et al., 2015). The positive results regarding the collagen type II consistent with a study of Bach *et al* 2016 and 2015, suggesting that NCCM induced collagen type II deposition (Bach et al., 2015; Bach et al., 2016). In our study, collagen type II deposition was highest after 2x NCM treatment, which suggests that this treatment may have the most regenerative effect of all treatment groups. In our study, the results indicate fibrosis and hypertrophic differentiation (Rutges, J P H J et al., 2010; Yee et al., 2016). are not present, and that healthy NP tissue was deposited.

Conclusion and future perspectives

The hypothesis of the current study was that NCM treatment would show a regenerative effect at MRI (T1ρ, T2 mapping, DHI) and protein expression level (collagen type I, II and X) and that MSC treatment could exert an additive effect.

The current stucy demonstrates that NCM reinjection improved the DHI and induced healthy ECM production. However, NCM treatment does not show a regenerative effect at quantitative T1ρ and T2 mapping. MSC treatment does not exert an additive effect.

We measured DHI, T1ρ and T2 mapping six weeks after induction of IVD degeneration. We knew what the values were at the beginning of the treatment and we were able to compare this with the results we had obtained after six months. In this way, the process can be followed closely and effects are more likely to be detected. However, it is recommended to perform an MRI at T= -1,5 months to know the values directly after induction of the IVDs without the treatments.

In our present study, we had a limited number of donors and also the sensitivity of the MRI is questionable.
Future studies are needed to evaluate the sensitivity of T2 and T1ρ mapping in degenerated IVDs and also in combination with regenerated IVDs.

References

Arkesteijn, I. I., Smolders, L. A., Spillekom, S., Riemers, F. M., Potier, E. E., Meij, B. P., . . . Tryfonidou, M. A. (2015). Effect of coculturing canine notochordal, nucleus pulposus and mesenchymal stromal cells for intervertebral disc regeneration. *Arthritis Research & Therapy, 17*(1), 60. doi:10.1186/s13075-015-0569-6

Bach, F. C., de Vries, S. A., Krouwels, A., Creemers, L. B., Ito, K., Meij, B. P., & Tryfonidou, M. A. (2015). The species-specific regenerative effects of notochordal cell-conditioned medium on chondrocyte-like cells derived from degenerated human intervertebral discs. *European Cells & Materials [E], 30*, 132. Retrieved from http://www.narcis.nl/publication/RecordID/oai:dspace.library.uu.nl:1874%2F327195

Bach, F. C., de Vries, S. A., Riemers, F. M., Boere, J., van Heel, F. W., van Doeselaar, M., . . . Tryfonidou, M. A. (2016). Soluble and pelletable factors in porcine, canine and human notochordal cell-conditioned medium: Implications for IVD regeneration. *European Cells & Materials, 32*, 163-180. doi:10.22203/eCM.v032a11

Bach, F. C., Willems, N., Penning, L. C., Ito, K., Meij, B. P., & Tryfonidou, M. A. (2014). Potential regenerative treatment strategies for intervertebral disc degeneration in dogs. *BMC Veterinary Research, 10*(1), 3. doi:10.1186/1746-6148-10-3

Bergknut, N., Grinwis, G., Pickee, E., Auriemma, E., Lagerstedt, A., Hagman, R., . . . Meij, B. (2011). Reliability of macroscopic grading of intervertebral disk degeneration in dogs by use of the thompson system and comparison with low-field magnetic resonance imaging findings. *American Journal of Veterinary Research, 72*(7), 899-904. doi:10.2460/ajvr.72.7.899

Bergknut, N., Smolders, L. A., Grinwis, G. C. M., Hagman, R., Lagerstedt, A., Hazewinkel, H. A. W., . . . Meij, B. P. (2013). Intervertebral disc degeneration in the dog. part 1: Anatomy and physiology of the intervertebral disc and characteristics of intervertebral disc degeneration. *Veterinary Journal (London, England : 1997), 195*(3), 282. doi:10.1016/j.tvjl.2012.10.024

de Vries, S. A. H., Potier, E., van Doeselaar, M., Meij, B. P., Tryfonidou, M. A., & Ito, K. (2015). Conditioned medium derived from notochordal cell-rich nucleus pulposus tissue stimulates matrix production by canine nucleus pulposus cells and bone marrow-derived stromal cells. *Tissue Engineering Part A, 21*(5-6), 177-1084. doi:10.1089/ten.tea.2014.0309

Ellis, P. (2012). *Effect size matters: How reporting and interpreting* MadMethods: Kingpress.org.

effect sizes can improve your publication prospect
s and change
the world!

Ganey, T., Hutton, W., Moseley, T., Hedrick, M., & Meisel, H. (2009). Intervertebral disc repair using adipose tissue-derived stem and regenerative cells: Experiments in a canine model. *Spine (Philadelphia, Pa.1976), 34*(21), 2297-2304. doi:10.1097/BRS.0b013e3181a54157

Greenland, S., Senn, S., Rothman, K., Carlin, J., Poole, C., Goodman, S., & Altman, D. (2016). Statistical tests, P values, confidence intervals, and power: A guide to misinterpretations. *European Journal of Epidemiology, 31*(4), 337-350. doi:10.1007/s10654-016-0149-3

Hiyama, A., Mochida, J., Iwashina, T., Omi, H., Watanabe, T., Serigano, K., . . . Sakai, D. (2008). Transplantation of mesenchymal stem cells in a canine disc degeneration model. *Journal of Orthopaedic Research, 26*(5), 589-600. doi:10.1002/jor.20584

Johannessen, W., Auerbach, J., Wheaton, A., Kurji, A., Borthakur, A., Reddy, R., & Elliott, D. (2006). Assessment of human disc degeneration and proteoglycan content using T1rho-weighted magnetic resonance imaging. *Spine (Philadelphia, Pa.1976), 31*(11), 1253-1257. doi:10.1097/01.brs.0000217708.54880.51

Kranenburg, H. C., Grinwis, G. C. M., Bergknut, N., Gahrmann, N., Voorhout, G., Hazewinkel, H. A. W., & Meij, B. P. (2013). Intervertebral disc disease in dogs – part 2: Comparison of clinical, magnetic resonance imaging, and histological findings in 74 surgically treated dogs. *Veterinary Journal, 195*(2), 164. doi:10.1016/j.tvjl.2012.06.001

Masuda, K., Imai, Y., Okuma, M., Muehleman, C., Nakagawa, K., Akeda, K., . . . An, H. S. (2006). Osteogenic protein-1 injection into a degenerated disc induces the restoration of disc height and structural changes in the rabbit anular puncture model. *Spine, 31*(7), 742-754. doi:10.1097/01.brs.0000206358.66412.7b

Phinney, D. (2012). Functional heterogeneity of mesenchymal stem cells: Implications for cell therapy. *Journal of Cellular Biochemistry, 113*(9), 2806-2812. doi:10.1002/jcb.24166

Richardson, S. M., Kalamegam, G., Pushparaj, P. N., Matta, C., Memic, A., Khademhosseini, A., . . . Hoyland, J. A. (2016). Mesenchymal stem cells in regenerative medicine: Focus on articular cartilage and intervertebral disc regeneration. *Methods, 99*, 69-80. doi:10.1016/j.ymeth.2015.09.015

Rutges, J P H J, Duit, R. A., Kummer, J. A., Oner, F. C., van Rijen, M. H., Verbout, A. J., . . . Creemers, L. B. (2010). Hypertrophic differentiation and calcification during intervertebral disc degeneration. *Osteoarthritis and Cartilage, 18*(11), 1487-1495. doi:10.1016/j.joca.2010.08.006

Sakai, D., Mochida, J., Iwashina, T., Hiyama, A., Omi, H., Imai, M., . . . Hotta, T. (2006). Regenerative effects of transplanting mesenchymal stem cells embedded in atelocollagen to the degenerated intervertebral disc. *Biomaterials, 27*(3), 335-345. doi:10.1016/j.biomaterials.2005.06.038

Serigano, K., Sakai, D., Hiyama, A., Tamura, F., Tanaka, M., & Mochida, J. (2010). Effect of cell number on mesenchymal stem cell transplantation in a canine disc degeneration model. *Journal of Orthopaedic Research : Official Publication of the Orthopaedic Research Society, 28*(10), 1267-1275. doi:10.1002/jor.21147

Smolders, L. A., Bergknut, N., Grinwis, G. C. M., Hagman, R., Lagerstedt, A. S., Hazewinkel, H. A. W., . . . Meij, B. P. (2013). Intervertebral disc degeneration in the dog. part 2: Chondrodystrophic and non-chondrodystrophic breeds. *Veterinary Journal, 195*(3), 292. doi:10.1016/j.tvjl.2012.10.011

Smolders, L., Meij, B., Onis, D., Riemers, F., Bergknut, N., Wubbolts, R., . . . Tryfonidou, M. (2013). Gene expression profiling of early intervertebral disc degeneration reveals a down-regulation of canonical wnt signaling and caveolin-1 expression: Implications for development of regenerative strategies. *Arthritis Research & Therapy, 15*(1), R23. doi:10.1186/ar4157

Steffen, F., Smolders, L., Roentgen, A., Bertolo, A., & Stoyanov, J. (2017). Bone marrow-derived mesenchymal stem cells as autologous therapy in dogs with naturally occurring intervertebral disc disease: Feasibility, safety and preliminary results. *Tissue Engineering Part C: Methods,* doi:10.1089/ten.TEC.2017.0033

Sun, W., Zhang, K., Zhao, C., Ding, W., Yuan, J., Sun, Q., . . . Zhao, J. (2013). Quantitative T2 mapping to characterize the process of intervertebral disc degeneration in a rabbit model. *BMC Musculoskeletal Disorders, 14*(1), 357. doi:10.1186/1471-2474-14-357

Thrall, D. E. (2013). *Textbook of veterinary diagnostic radiology* (6. ed. ed.). St. Louis, Mo: Elsevier.

Vargha, A. (2000). A critique and improvement of the CL common language effect size statistics of McGraw and wong. *Journal of Educational and Behavioral Statistics, 25*(2), 101-132.

Willems, N., Bach, F. C., Plomp, S. G. M., van Rijen, Mattie H P, Wolfswinkel, J., Grinwis, G. C. M., . . . Tryfonidou, M. A. (2015). Intradiscal application of rhBMP-7 does not induce regeneration in a canine model of spontaneous intervertebral disc degeneration. *Arthritis Research & Therapy, 17*, 137. Retrieved from http://www.ncbi.nlm.nih.gov/pubmed/26013758

Willems, N., Tellegen, A., Bergknut, N., Creemers, L., Wolfswinkel, J., Freudigmann, C., . . . Meij, B. (2016). Inflammatory profiles in canine intervertebral disc degeneration. *BMC Veterinary Research, 12*, 10. doi:10.1186/s12917-016-0635-6

Yee, A., Lam, M. P. Y., Tam, V., Chan, W. C. W., Chu, I. K., Cheah, K. S. E., . . . Chan, D. (2016). Fibrotic-like changes in degenerate human intervertebral discs revealed by quantitative proteomic analysis. *Osteoarthritis and Cartilage, 24*(3), 503-513. doi:10.1016/j.joca.2015.09.020

Zhang, Y., Hu, J., Duan, C., Hu, P., Lu, H., & Peng, X. (2017). Correlation study between facet joint cartilage and intervertebral discs in early lumbar vertebral degeneration using T2, T2* and T1 ρ mapping. *PLoS One, 12*(6), e0178406. doi:10.1371/journal.pone.0178406